Available online at www.sciencedirect.com
ScienceDirect
Developmental Biology 301 (2007) 388–403
DEVELOPMENTAL BIOLOGY
www.elsevier.com/locate/ydbio

Coordination of symmetric cyclic gene expression during somitogenesis by Suppressor of Hairless involves regulation of retinoic acid catabolism

Karen Echeverri [1], Andrew C. Oates *

Max Planck Institute for Molecular Cell Biology and Genetics, Pfotenhauerstr 108, 01307 Dresden, Germany

Received for publication 11 May 2006; revised 29 September 2006; accepted 5 October 2006
Available online 10 October 2006

Abstract

Vertebrate embryos faithfully produce bilaterally symmetric somites that give rise to repetitive body structures such as vertebrae and skeletal muscle. Body segmentation is regulated by a cyclic gene expression system, containing the Delta–Notch pathway and targets, which generates bilaterally symmetric oscillations across the Pre-Somitic Mesoderm (PSM). The position of the forming somite boundary is controlled by interaction of this oscillator with a determination front comprised of opposing gradients of FGF and retinoic acid (RA) signalling. Disruption of RA production leads to asymmetries in cyclic gene expression, but the link between RA and the oscillator is unknown. In somitogenesis, Notch signalling activates target genes through the transcription factor Suppressor of Hairless (Su(H)). Here, we report that two *Su(H)* genes coordinate bilaterally symmetric positioning of somite boundaries in the zebrafish embryo. Combined *Su(H)* gene knockdown caused defects in visceral left/right asymmetry, neurogenic lateral inhibition, and symmetrical failure of the segmentation oscillator. However, by selectively down-regulating *Su(H)2* or *Su(H)1* function using specific antisense morpholinos, we observed asymmetric defects in anterior or posterior somite boundaries, respectively. These morphological abnormalities were reflected by underlying asymmetric cyclic gene expression waves in the presomitic mesoderm, indicating a key role for *Su(H)* in coordinating the left–right symmetry of this process. Strikingly, expression of the RA-degrading enzyme *cyp26a1* in the tailbud was controlled by *Su(H)* activity, and morpholino knockdown of *cyp26a1* alone caused asymmetric cyclic *dlc* expression, suggesting that excess RA in the tailbud may contribute to the cyclic asymmetries. Indeed, exogenous RA was sufficient to generate asymmetric expression of all cyclic genes. Our observations indicate that one element of the Notch signalling pathway, Su(H), is required for control of RA metabolism in the tailbud and that this regulation is involved in bilateral symmetry of cyclic gene expression and somitogenesis.

Keywords: Somitogenesis; Notch signalling; Retinoic acid; Asymmetry; Segmentation; Zebrafish

Introduction

During embryogenesis the body axis is sequentially subdivided from head to tail into blocks of tissue called somites that give rise to repetitive structures such as the vertebrae, ribs and skeletal muscle. The somites bud from the anterior most end of the unsegmented Pre-Somitic Mesoderm (PSM), forming simultaneously and symmetrically on either side of the midline. The periodicity of this process is thought to be controlled by the combined action of a 'segmentation clock', a genetic oscillator that regulates the temporal and spatial organization of cells within the PSM, and a 'wavefront' or gradient that arrests the oscillations at a determination front (Palmeirim et al., 1997, 1998; Pourquie, 2001; Pourquie and Kusumi, 2001; Pourquie and Tam, 2001).

The first evidence of a segmentation oscillator came from work in chick demonstrating the oscillatory mRNA expression of the basic helix–loop–helix (bHLH) gene, c-*Hairy1* (Palmeirim et al., 1997). Expression initiates in the posterior-most PSM and travels anteriorly in a wave-like manner, arresting at the newly forming somite boundary (Masamizu et al., 2006). Subsequent work in mouse and zebrafish has shown that these species also possess several so-called cyclic genes with almost identical wave-like mRNA expression patterns in the PSM (Aulehla and Johnson, 1999; Aulehla et al., 2003; Holley et al., 2000, 2002; Jiang et al., 2000; Jouve et al., 2000; Oates and Ho, 2002). To

* Corresponding author.
E-mail address: oates@mpi-cbg.de (A.C. Oates).
[1] Current address: DFG Research Centre for Regenerative Therapies Dresden, c/o BIOTEChnology Center, Dresden University of Technology, Tatzberg 47-51, 01307 Dresden, Germany.

0012-1606/$ - see front matter © 2006 Elsevier Inc. All rights reserved.
doi:10.1016/j.ydbio.2006.10.003

date, almost all identified cyclic genes are involved in the Delta/Notch intercellular signalling pathway. Importantly, somite formation and wave-like expression patterns of most cyclic genes are disrupted by mutations or perturbations in this pathway (Aulehla et al., 2003; Barrantes et al., 1999; Bessho et al., 2001b; Dunwoodie et al., 2002; Evrard et al., 1998; Holley et al., 2000, 2002; Jiang et al., 2000; Jouve et al., 2000; Julich et al., 2005; Koizumi et al., 2001; Morales et al., 2002; Oates and Ho, 2002; Sieger et al., 2003; Zhang and Gridley, 1998).

Notch mediated cell-to-cell signalling is widely used by vertebrates to specify cell fate and regulate pattern formation. Binding of Notch to its ligand, Delta or Serrate, on a neighboring cell causes the intracellular domain of Notch to be proteolytically cleaved. The Notch intracellular domain (NICD) then translocates into the nucleus where it associates with the highly conserved DNA binding protein Suppressor of Hairless Su(H)/RBPJk and converts the latter from a transcriptional repressor to a transcriptional activator (reviewed in Schweisguth, 2004). Downstream target genes transcriptionally activated by the NICD–Su(H) complex include members of the Hairy family of genes, themselves known to encode transcriptional repressors, raising the possibility that a transcriptional feedback loop might be part of the oscillator mechanism (Bessho et al., 2003; Hirata et al., 2002; Palmeirim et al., 1997). Cyclic *hairy* homologues have been identified in the chick and mouse PSM (Bessho et al., 2001a; Jouve et al., 2000; Leimeister et al., 2000; Li et al., 2003), and in zebrafish, the *Hairy* homologues *her1*, *her7*, *her11* and *her12* display oscillating expression (Holley et al., 2000, 2002; Oates and Ho, 2002; Sawada et al., 2000; Sieger et al., 2004; Gajewski et al., 2006). This suggests a conserved role for the *Hairy* family in the somitogenesis oscillator.

Evidence from different vertebrate embryos suggest that a critical event in the oscillator is periodic Notch activation, even though the molecular means of achieving this end may vary between species. Expression of the Notch ligand *deltaC* (*dlc*) is cyclic in the zebrafish, but no known Delta genes cycle in the PSM of mouse or chick. Instead, expression of the glycosyl-transferase *lunatic fringe*, which itself has been identified as a modulator of Notch signaling, is cyclicly transcribed in mouse and chick (Forsberg et al., 1998; McGrew et al., 1998; Morales et al., 2002; Prince et al., 2001). To date, no oscillating *lunatic fringe* homologue has been identified in zebrafish (Prince et al., 2001; Leve et al., 2001). Recent studies in mouse have also found two oscillating members of the canonical Wnt pathway (Aulehla et al., 2003; Ishikawa et al., 2004) although no Wnt pathway gene has been found to oscillate in the zebrafish. Thus, the emerging model of the oscillator in the zebrafish is of a genetic feedback mechanism consisting of components of the Delta/Notch signaling pathway and their target genes, which causes the cells of the PSM to undergo repeated cycles of gene expression and repression. In amniotes Wnt signalling also appears to be involved (reviewed in Aulehla and Herrmann, 2004).

The determination front, initially defined by a series of elegant transplantation studies, is the position in the PSM at which cells respond to the periodic signals of the oscillator and thereby determine the position of the future segmental boundaries (reviewed in Dubrulle and Pourquie, 2004a; Aulehla and Herrmann, 2004). The size of a somite is thus given by the number of cells experiencing the transit of the determination front during one cycle of the segmentation oscillator. The A/P positioning of the determination front within the PSM is thought to be controlled by two opposing and interacting gradients of FGF and retinoic acid (RA). Highest in the posterior, a gradient of FGF signalling creates a threshold that acts as the signal to the PSM cells to arrest oscillations at the determination front (Sawada et al., 2001; Dubrulle et al., 2001; Dubrulle and Pourquie, 2004b), and Wnt signalling may also contribute to this arrest (Aulehla et al., 2003). From the anterior, a gradient of retinoic acid (RA) can also alter the position of the determination front by antagonizing FGF signalling (Diez del Corral et al., 2003; Moreno and Kintner, 2004). Although in *Xenopus* the FGF-signal transduction inhibitory phosphatase MKP3 is involved in establishing the position of the determination front (Moreno and Kintner, 2004), the mechanism of interaction of the gradients in the PSM of different species is still unclear. Control of FGF concentration in the mouse PSM is regulated by mRNA stability in cells emerging from the tailbud (Dubrulle and Pourquie, 2004b), whereas RA levels are set by the balance of RA anabolism in the somites (the source) through Raldh2, the last enzyme in the synthesis pathway, and catabolism via Cyp26a, expressed in the tailbud (the sink). The establishment of opposing FGF and RA gradients by somites and tailbud may be a general mechanism to sharpen a determination or differentiation front in a growing tissue (reviewed in (Diez del Corral et al., 2003). We note that a RA-independent mechanism involving *her13.2* in the zebrafish has been proposed to control the determination front (Kawamura et al., 2005), suggesting additional complexities in the regulation of the system.

Recent reports have shown a dramatic loss of bilateral coordination of symmetric cyclic gene expression following reduction of RA production in chick, mouse and zebrafish embryos (Kawakami et al., 2005; Sirbu and Duester, 2006; Vermot et al., 2005; Vermot and Pourquie, 2005), and in chick, an asymmetry in the final positions of somite boundaries. It was therefore proposed that the RA gradient might act additionally to, or through its role in determination front positioning, as a buffer to prevent asymmetric signalling molecules involved in visceral laterality from perturbing the bilateral synchrony of the segmentation oscillator (Brent, 2005; Hornstein and Tabin, 2005). Importantly, in all determination front-based models (Dubrulle and Pourquie, 2002), the segmentation oscillator is downstream of, or constrained by these gradients; to date there is no evidence that the segmentation oscillator plays a role in setting the shape, amplitude, or interactions of the FGF or RA gradients.

Here we report that the function of duplicated Su(H) genes, encoding the critical transcriptional mediators of Notch signalling, are required for symmetric cyclic gene expression in zebrafish. Surprisingly, *Su(H)* function is required for expression of *cyp26a1*, the gene which encodes the RA catabolic enzyme in the tailbud, and that is in turn necessary for cyclic *dlc* expression. Consistent with the loss of a catabolic sink for RA in the affected embryos, increasing levels of exogenous RA induces cyclic gene expression asymmetries. These results show for the first time a

direct connection between a component of the somitogenesis oscillator and the RA pathway.

Materials and methods

Fish care

Fish were kept on a 14 h light/10 h dark light cycle following standard culture methods and were staged according to (Kimmel et al., 1995). Fish strains AB or Gol were used for all experiments.

Cloning of two Suppressor of Hairless genes

Using a nesting strategy with degenerate primers, two different *Su(H)* transcripts were isolated from *Danio rerio* cDNA. All PCR was performed with the profile: 5 min at 95°C, then 30 cycles of 30 s at 95°C, 1 min at 55°C, 1 min at 72°C, then 10 min at 72°C. In the first round of amplification, SuH1: GCI CA(AG) AA(AG) (AT)(GC)I TA(CT) GGI AA(CT) GA and SuH3R: CCA I(GC)(AT) IGC ICC (AG)TC (AG)TT IAT CAT were used to generate template from embryonic cDNA for a second round using SuH2: CA(AG) (CT)TI CA (CT) AA(AG) TG(CT) GCI TT(CT) TA and SuH3R, where I denotes an Inosine residue. A 120 bp PCR product was isolated after electrophoresis, subcloned and found to contain two distinct *Su(H)*-related gene fragments assessed by BLAST search against the zebrafish Ensembl and NCBI databases. 5′ and 3′ RACE PCR was used to complete the cDNAs. One cDNA corresponds to the previously identified *Su(H)* gene (Sieger et al., 2003), termed rbpsuh from ENSDARG00000003398 on Chromosome 1 at 15.6. The newly identified cDNA is described as a novel gene ENSDARG00000052091 on Chromosome 7 at 62.0 (Ensembl v37). We have submitted our cDNA sequences to NCBI.

Intron-derived riboprobes

Genomic DNA from the *Su(H)1* and *Su(H)2* genes was amplified using primers designed to avoid regions of high nucleotide similarity between potential exons as follows: csl1-1 TGTTCTACGGTAATAGCGCAG; csl1-2R GTCTGCTTGTCCACTTTACGA; csl2-4 CACTACGGACAAACTGTCAAA; csl2-2R GTCTGCTTATCCACCTTACGG, yielding products of 1.5 and 1.3 kb respectively. These primer pairs were used to map the *Su(H)1* and *Su(H)2* genes to LG1 with a LOD of 14.0, and LG7 with a LOD of 8.1, respectively, on the LN54 radiation hybrid panel (Hukriede et al., 1999). Three introns were found in the *Su(H)1* product and one in the *Su(H)2* product such that overall these sequences were 66% and 93% intron-derived. After subcloning, these fragments were used to generate riboprobes for in situ hybridization (see below).

Morpholino design and injection

Antisense morpholino oligonucleotides complementary to the 5′ regions of *Su(H)1* and *Su(H)2*, and a morpholino targeting the ATG of both *Su(H)* genes were designed and synthesised by Gene Tools LLC (Philomath, Oregon). Su(H) 1 MO: 5′-CCG GTG TGA CAA ATA ACG CCA GGA A-3′; Su(H)2 MO1: 5′-CGC CAT CTT CCA CAA ACT CTC ACC A-3′; Su(H)2 MO2: 5′-TCC TCC TCT CCC AGA CCC TTC CAG C-3′; Su(H)1+2 MO: CAA ACT TCC CTG TCA CAA CAG G-3′. The standard control MO recommended by Gene Tools was: 5′-CCT CTT ACC TCA GTT ACA ATT TAT A-3′. The same antisense morpholino for *cyp26a1* was used as previously described by Emoto et al. (2005) and with the same amount injected (1 ng): cyp26a1 MO: 5′-CGC GCA ACT GAT CGC CAA AAC GAA A-3′. Morpholinos were resuspended in distilled water, then diluted to 10 ng/μL in 1× Danieau's solution and stored at −20°C. Prior to injection morpholinos were further diluted to the following optimized concentrations in 1× Danieau's plus 0.2 mg/mL Fast Green: *Su(H)1* was targeted with Su(H)1 MO at 7 ng; Su(H)2 was targeted with 1 ng of Su(H)2 MO1 and 1 ng of Su(H)2 MO2; the Su(H)1+2 MO targeting both transcripts (equivalent to the ORF-MO of Sieger et al., 2003) was used at 7 ng; and to target both transcripts independently, Su(H)1 MO at 5 ng was combined with Su(H)2 MO1 and Su(H)2 MO2 at 0.5 ng each. The independent Su(H)2 MOs gave indistinguishable results, but with a low percentage of affected embryos. Therefore, both Su(H)2 MOs were co-injected to increase the penetrance, and are used in combination throughout the results, unless otherwise stated (see Table 1). Morpholinos were injected into the embryo at the one cell stage.

Retinoic acid treatment

All trans retinoic acid (RA, Sigma) was dissolved in DMSO to make a stock solution of 10 mM. This was then diluted in E3 medium to give a final concentration of 10^{-9}, 10^{-12} or 10^{-15} M RA. Embryos were incubated in their chorions in the solution containing RA from tailbud stage to the time point at which they were fixed for analysis.

mRNA synthesis and injection

Capped RNA was synthesized from Dominant Active (DA) *Suppressor of Hairless* expression construct in pCS2+ vector (gift from David Wilkinson's lab, NIMR, London) using the mMessage mMachine SP6 transcription kit (Ambion). Full length coding sequence of the *Su(H)1* and *Su(H)2* cDNAs lacking 5′ or 3′ UTRs were subcloned into pCS2+ for expression in the embryos. One cell stage zebrafish embryos were pressure injected with the RNA diluted to 0.2–1 μg/μl in 0.1 M KCL plus 0.2 mg/mL Fast Green as tracer dye.

In situ hybridizations

In situ hybridizations were carried out as previously described (Oates and Ho, 2002), and double in situs were performed as described by Prince et al. (1998). The riboprobes were generated from plasmids as already described: *her1*, *her7*, *dlc*, *titin* (Oates and Ho, 2002). The *cmcl2* and *cyp26a1* plasmids were from the labs of S. Abdelilah and M. Brand respectively. Riboprobes transcribed from the Su(H) genomic clones described above were used with annealing temperatures of 50°C.

Antibody staining

10–15 somite stage embryos were fixed overnight in 4% PFA, and washed briefly in PBST, followed by 3×15 min in PBS containing DMSO and 0.1% Triton X-100. Embryos were then blocked at room temperature for 1 h in PBST containing BSA and 10% goat serum. The embryos were incubated overnight in primary anti-fibronectin antibody (Sigma) diluted 1:500 into block solution. Embryos were washed 4×15 min in PBST and then incubated in secondary antibody for 1 h at room temperature. Embryos were then washed in PBST, incubated for 15 min in PBST plus Hoechst 33342, rinsed briefly and transferred into a solution of 80% glycerol for deyolking and flat-mounted for imaging on a Zeiss confocal LSM.

Results

A second active Suppressor of Hairless gene in zebrafish

Previous work established the existence of a zebrafish homolog of the CBF1/Su(H)/Lag-1 family termed *Su(H)*

Table 1
Summary of phenotypes observed at 24 hpf in embryos with compromised *Su(H)* function

Morpholino injected	Concentration of MO injected (ng/nl)	Anterior defects (%)	Posterior defects (%)	Heart defects (%)	Total number of embryos
Su(H)1 MO	7	0	72	70	90
Su(H)2 MO1+MO2	1+1	75	75	72	100
Su(H)1MO+Su(H)2 MOs	5+1+1	80	80	90	120
Su(H)1+2 MO	7	65	65	70	70

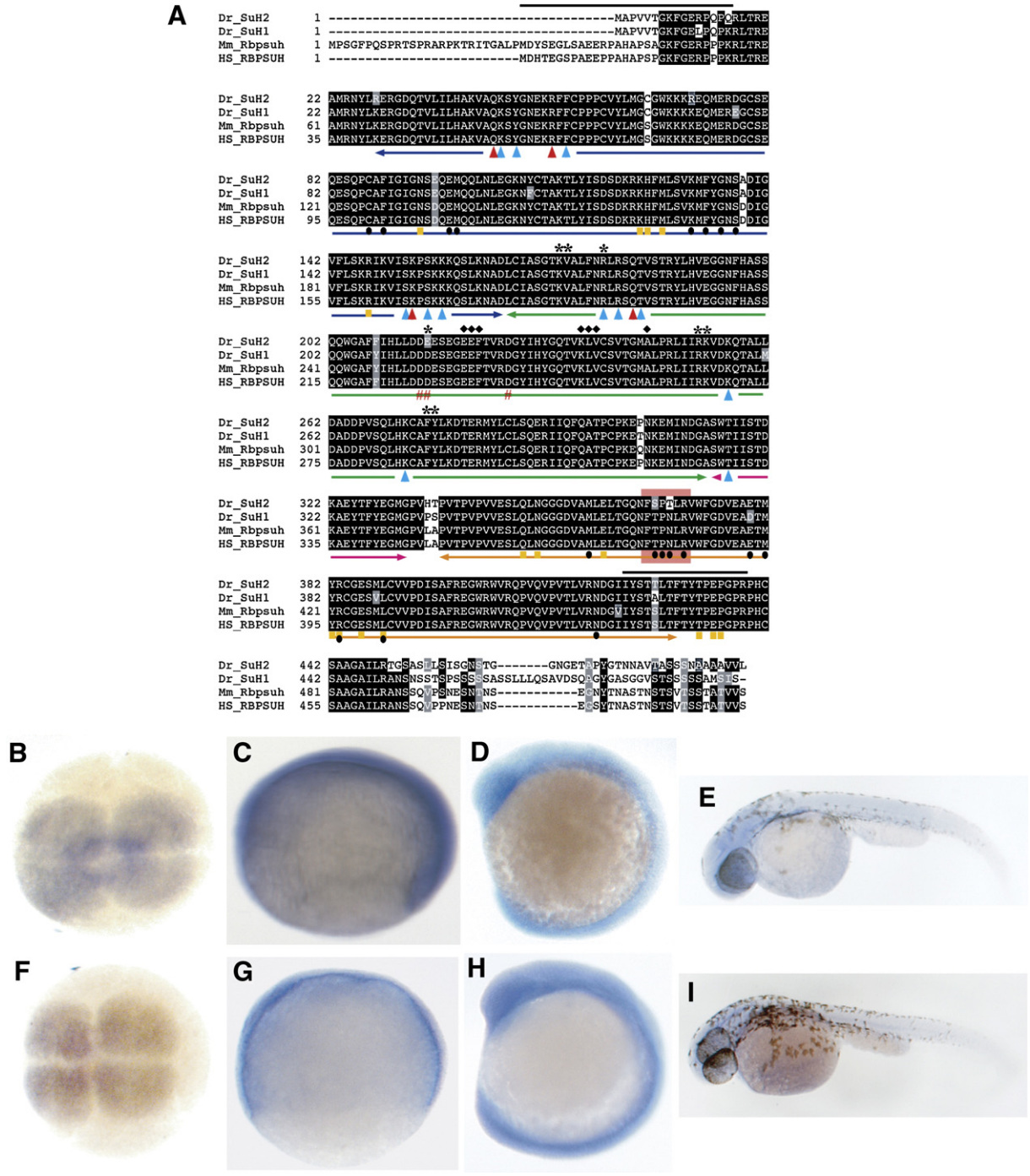

Fig. 1. Structure and expression of the duplicate zebrafish *Su(H)* genes. (A) Peptide sequences of zebrafish Su(H)1 and Su(H)2 aligned with mouse and human (Mm and Hs) proteins using the ClustalW WWW Service at the European Bioinformatics Institute (http://www.ebi.ac.uk/clustalw; Thompson et al., 1994). Colored horizontal arrows and vertical arrowheads below the alignment demarcate the 3D arrangement of the peptide, and the peptide–DNA contact points, respectively, as determined by crystal structure of Lag-1 (Kovall and Hendrickson, 2004). Blue arrows—N-terminal domain (NTD, Rel Homology Region-N); green arrows—beta-trefoil domain; magenta arrow-βc4 strand; orange arrows C-terminal domain (CTD, Rel Homology Region-C). Red arrowheads—sequence specific contacts to DNA base pairs; light blue—contacts to backbone. Residues contacting the NICD ANK domain and the MAM peptide, as determined by crystal structure, are indicated by yellow squares and black circles respectively below the alignment (Nam et al., 2006; Wilson and Kovall, 2006). Electronegative patch residues involved in RAM interaction are marked with red hash (#) symbols (Wilson and Kovall, 2006). Residues and regions functionally implicated in interactions with other proteins by deletion or mutational studies are marked in black above the alignment. Asterisks mark residues involved in binding NICD through the RAM domain (Fuchs et al., 2001; Sakai et al., 1998). Black bars indicate regions required to bind co-activator MAML in complex with NICD (Nam et al., 2003). Residues involved in binding RAM and co-repressors CIR and SMRT are highlighted by black diamonds (Fuchs et al., 2001; Hsieh et al., 1999). Note the sequence variation in Su(H)2 in the MAM-binding interface (S376, T378) highlighted by the red rectangle, and the highly divergent C-terminal 45–50 amino acids. (B) Whole mount in situ hybridization of maternal *Su(H)1* transcript at the 4 cell stage. (C) After mid-blastula transition, putative zygotic transcript is detected throughout the embryo at 70% epiboly (C), 10 somite stage (D), and 30–36 h post fertilization (hpf) (E). (F–I) Expression of the *Su(H)2* transcript through the same stages of development is indistinguishable.

(Sieger et al., 2003). We isolated this gene and a second homolog using a degenerate primer PCR protocol (see materials and methods). The duplicated zebrafish genes, which we term *Su(H)1* (Sieger et al., 2003) and *Su(H)2*, are themselves highly conserved, with their proteins showing 90% amino acid identity overall (Fig. 1A). In contrast, a C-terminal serine-rich domain (45–50 aa) is highly diverged: whereas mouse and human proteins are 95% identical in this domain, Su(H)1 and Su(H)2 share only 17% identity, and only 3 residues are conserved between all four proteins. Comparison of our *Su(H)1* and *Su(H)2* cDNA sequences to the Ensembl v37 zebrafish genome assembly, and PCR amplification of gene-specific intron sequences demonstrates unequivocally that they are distinct genes (data not shown). Analysis of mRNA expression by in situ hybridization shows that both transcripts are maternally provided (Figs. 1B,F) and detectable throughout the embryo until around 24 h post fertilization (hpf), beyond which point both transcripts become restricted to the head (Figs. 1E,I). To control for possible cross hybridization between cDNA-derived probes and *Su(H)* target mRNA due to very high nucleotide similarity between the Su(H)1 and Su(H)2 transcripts, we performed additional experiments with riboprobes derived from unique intron sequences from each gene, but did not detect any differences (data not shown). These expression results confirm those of Sieger et al. (2003) for *Su(H)1* and indicate that *Su(H)1* and *Su(H)2* are co-expressed throughout the first day of development.

Su(H)1 and Su(H)2 in neurogenesis and heart development and laterality

Finding two highly conserved *Su(H)* genes co-expressed throughout the embryo raises the hypothesis that they may both be required in a given cell to mediate normal levels of Notch signal transduction. Alternatively, they may be completely redundant, and only a loss of both *Su(H)* functions will cause a loss of Notch signalling competence. We examined the 5′ sequence of each *Su(H)* gene and found that the previously used antisense morpholino reagents (Sieger et al., 2003) do not distinguish between these highly similar transcripts, raising the possibility that both genes were inadvertently targeted in that study (Supplementary Figure S1). Before turning our attention to the implications of this observation for somitogenesis, we tested our hypothesis in two independent developmental contexts where Notch signalling is known to be important. We first injected morpholinos targeted to distinct regions of *Su(H)1* and *Su(H)2*, both alone and in combination, and examined their effect on the process of lateral inhibition, a pathway well documented in zebrafish and other animals to be regulated via the Notch signalling pathway (Appel and Eisen, 1998a; Inoue et al., 1994). When either of the two *Su(H)* genes are down-regulated we observe that an excess of Rohon–Beard neurons are made throughout the neural axis, as identified by *islet1* expression and their position in the CNS (Figs. 2B,C). When both genes are down-regulated we see a much more extensive number of neurons, including Rohon–Beard, ventral motor neurons, and also an enlargement of the trigeminal ganglia along the DV axis (Figs. 2D,F), suggesting an additive role for *Su(H)* genes during neurogenesis. This effect is highly similar to that seen in a *mindbomb* mutant, which exhibits the strongest known Notch-related neurogenic phenotype (Jiang et al., 1996; Itoh et al., 2003). This experiment indicates that knockdown of either individual *Su(H)* gene does not match the phenotypic strength of a loss of Notch signalling, whereas a reduction of both *Su(H)* functions does.

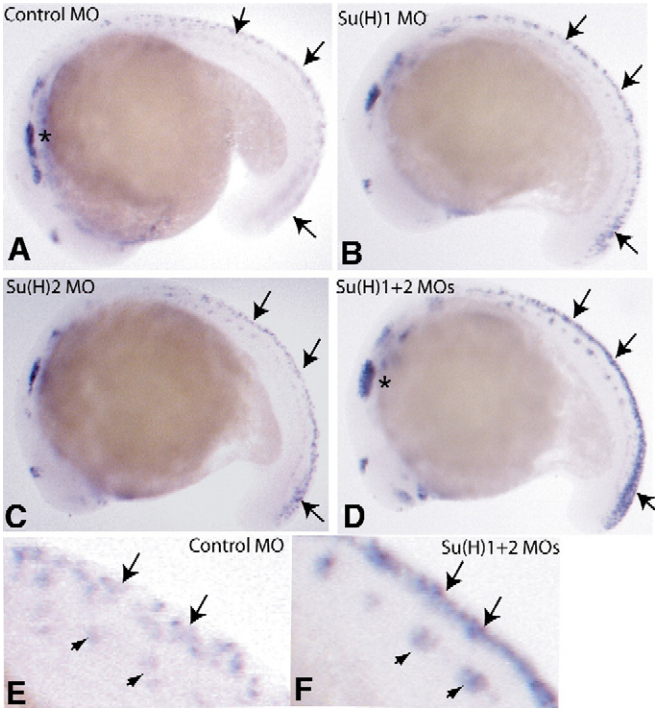

Fig. 2. Increased *Islet1* expression in *Su(H)* morphant embryos. (A–D) Lateral view of whole mount 15–20 somite stage embryos. (A) Control morpholino (MO)-injected embryo: *islet1* is expressed most prominently in the dorsal Rohon–Beard neurons along the spinal cord (arrows), and in the trigeminal ganglion in the head (asterisk) ($n=40$). (B, C) Increase in Rohon–Beard neurons (arrows) observed along the neural axis in *Su(H)1* or *Su(H)2* morphant embryos (75%, $n=60$ for each MO). (D) Combined Su(H)1 and Su(H)2 MO-injected embryos display further increased neurogenesis in trigeminal ganglia (asterisk) and throughout the body axis, as indicated by arrows and arrowheads (80%, $n=60$). (E, F) Higher magnification images of the spinal cord showing Rohon–Beard neurons (arrows), and ventral primary motor neurons (arrowheads) in the control MO-injected (E), and combined *Su(H)* morphant embryo (F).

Notch signalling has also been implicated in the early establishment of left–right asymmetry in the viscera of chick, mouse and zebrafish embryos, the outcome of which can be accurately monitored by following the situs of the developing heart (Przemeck et al., 2003; Krebs et al., 2003; Raya et al., 2003; Kawakami et al., 2005). We therefore next compared the effect of knocking down the individual *Su(H)* genes with that of a combined knockdown on heart development and looping. In embryos with impaired functioning of the *Su(H)1* or *Su(H)2* gene, 30% display defects in elongation of the heart tube (Figs. 3B,E), 50% have defects in the heart primordium migrating from the midline (Figs. 3C,F), and 20% have a normal heart as judged by position, morphology, and expression of *cardiac myosin light chain* (*cmlc*, Fig. 3D). Thus loss of only

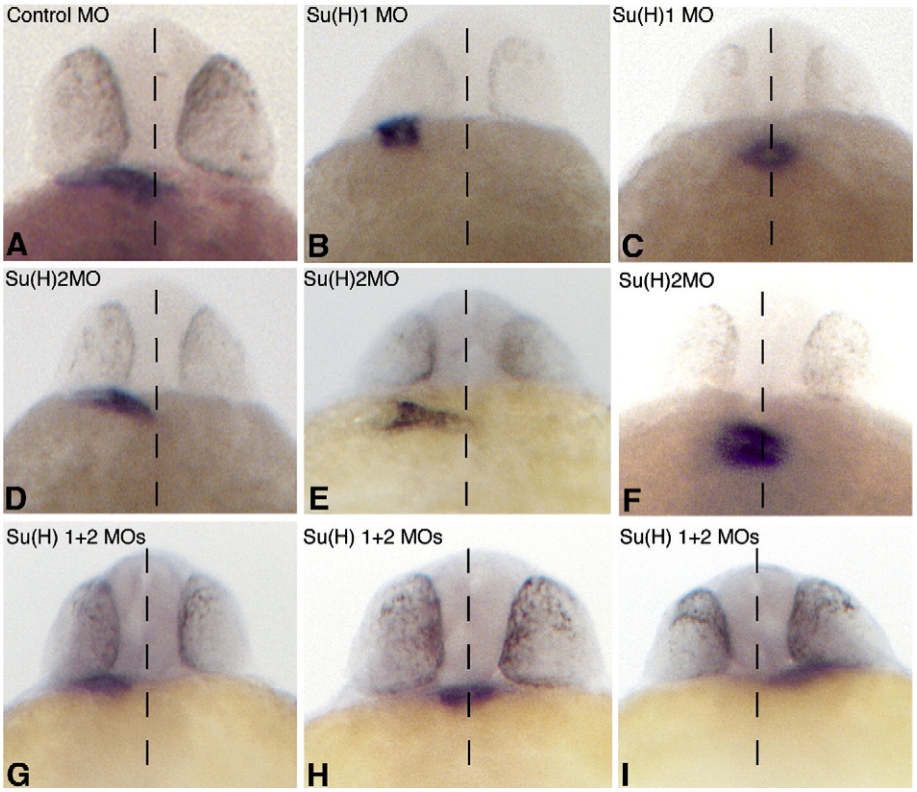

Fig. 3. Abnormal *cardiac myosin light chain* (*cmlc*) expression in *Su(H)* morphant embryos. (A) Dorsal view of control MO-injected embryo at 24 hpf: heart tube is positioned correctly on the left hand side ($n=50$). (B–F) In *Su(H)1* or *Su(H)2* morphant embryos, defects in elongation and positioning of the heart tube are seen in 30% of embryos (B, E). 50% embryos fail during the process of migration of the heart primordium from the midline (C, F) and 20% of embryos appear to have a normal heart (D). Su(H)1, MO $n=90$; Su(H)2 MO, $n=80$). (G–I) If both *Su(H)* genes are down-regulated, the position of the heart is randomised: (G) 20% left hand side, (H) 50% middle, (I) 30% right hand side ($n=90$).

a single *Su(H)* gene, reveals an apparently normal situs, but causes strong defects in heart tube maturation and subsequent movements. In contrast, when both *Su(H)* genes are down-regulated the position of the heart becomes randomised, being found on the right hand side in 30% of the embryos (Figs. 3G–I). Combined, these experiments indicate that in neurogenesis, heart development and laterality, a strong or complete Notch phenotype is only generated when both of the zebrafish *Su(H)* gene functions have been targeted, and that, depending on the developmental context examined, the individual *Su(H)* genes can play an additive role in the process.

Su(H)1 and Su(H)2 are involved in bilateral positioning of somite boundaries

To date, mutant and morpholino-generated somitogenesis phenotypes in the Notch signalling pathway have exhibited such profound morphological and molecular defects, that more subtle abnormalities such as asymmetries in boundary formation and cyclic expression patterns may have been overlooked. For example, loss of Notch1a, DeltaD, DeltaC or Mindbomb function in zebrafish leads to chaotic, partial boundary formation, and a complete and bilaterally symmetrical loss of cyclic expression waves (van Eeden et al., 1996; Holley et al., 2000, 2002; Jiang et al., 2000; Gajewski et al., 2003; Itoh et al., 2003; Oates and Ho, 2002; Oates et al., 2005). We reasoned that the additive nature of the duplicate *Su(H)* genes might offer a way to look at roles for Su(H) directly, and perhaps for Notch signalling in general, in the coordination of bilateral symmetry during somitogenesis.

Morpholinos were injected at the one cell stage and analysed at 24 h post fertilization (hpf) for defects in myotome boundaries marked by *titin* expression. Injection of the morpholino targeting *Su(H)1* produced defects only in the posterior body: from approximately somite boundary 9 onwards no clear myotome boundaries could be identified (Fig. 4B) and tail outgrowth was affected. From the *titin* staining it could be seen that the boundaries 1–9 form symmetrically without any apparent defects, a phenotype very similar to the known Delta/Notch mutants.

When morpholinos designed to target *Su(H)2* were injected singularly or combined in a lower dose, they produced defects in both anterior and posterior segment boundaries (Fig. 4C). The posterior boundaries were initially closer together and eventually the embryo stopped making boundaries altogether, concomitant with a mild tail outgrowth defect (Fig. 4C). The unusual nature of the anterior defects promoted us to examine them in more detail. Embryos stained for fibronectin accumulation clearly revealed asymmetric anterior boundary formation, as well as boundaries that did not span the entire mediolateral width of the somite (Figs. 4G–G″). In live *Su(H)2* morpholino injected embryos the somite boundaries in the anterior were

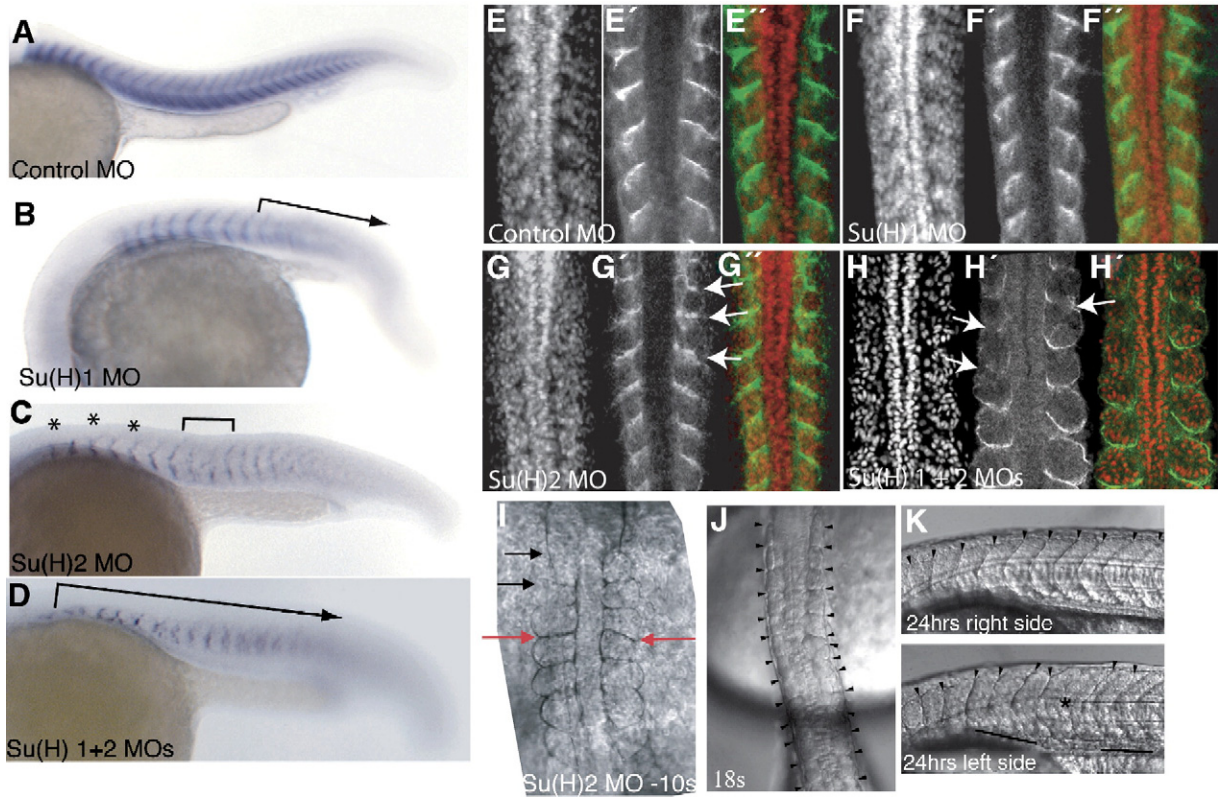

Fig. 4. Knockdown of *Su(H)* genes affects paraxial mesoderm segmentation. (A–D) Lateral view of 24 hpf embryos showing myotome boundaries marked by *titin* expression. (A) Control MO-injected embryo ($n=50$). (B) Su(H)1 MO-injected embryo: normal symmetric boundaries are formed up until boundary 8–10, as indicated by arrow. After this point, myotome boundaries are disrupted and tail outgrowth is abnormal (70%, $n=60$). (C) Su(H)2 MO-injected embryo: asterisk and bracket indicates where anterior boundaries are disrupted (75%, $n=70$). (D) Combined Su(H)1 and Su(H)2 MO-injected embryo showing additive effect of the single morphant embryos: anterior and posterior boundaries are affected and tail outgrowth is abnormal (85%, $n=70$). (E–H) Flat-mounted morpholino injected embryos at the 15 somite stage, showing anti-Fibronectin immunostaining of the anterior trunk somites: arrows indicate asymmetries, and missing or partial boundaries ($n=20$ for each MO), panels E–H shows nuclei stained with Hoechst 33342, panels E′–H′ shows Fibronectin immunostaining, and panels E″–H″ shows the overlay of nuclear Hoechst staining with Fibronectin localization for control MO (E–E″), Su(H)1 MO (F–F′), Su(H)2 MO (G–G″) and Su(H)1+2 MO (H–H″). (I–K) Development of abnormal anterior segment boundaries in live Su(H)2 MO-injected embryos. (I) Dorsal view of the first 6 somites in a live Su(H)2 morphant at the 10 somite stage, showing incomplete (black arrows) and asymmetric (red arrows) somite boundaries. (J) Dorsal view of live Su(H)2 morphant at the 18 somite stage showing asymmetric positioning of left and right-side somite boundaries (arrowheads). (K) Lateral view of the left and right sides of the anterior trunk of a Su(H)2 morphant at 24 hpf, showing regions of fused (asterisk) and incomplete (bars) myotome boundaries.

asymmetric or missing altogether (Figs. 4I–K), indicating that the abnormalities arose during somitogenesis, and were not the result of a later defect in myotome maturation. The asymmetries observed appeared to show no left or right sided bias within any clutch of embryos.

When morpholinos against *Su(H)1* and *Su(H)2* were co-injected and the embryos analysed at 24 hpf, we observed severe defects in boundaries along the entire axis of the embryo, with no consistent bias toward the left or right hand side observed, and a strong tail outgrowth phenotype (Fig. 4D). The defects are more severe than in embryos injected with Su(H)2 morpholino alone, indicating a function for the *Su(H)1* gene also in the anterior trunk. These results suggest that the somite phenotypes of the *Su(H)* genes are not simply additive, but may reflect a redundant biochemical function, or alternatively, participation in a parallel or robust mechanism.

The difference in morphological phenotype displayed by *Su(H)1* and *Su(H)2* knockdown embryos indicates the specificity of the morpholino targeting and action (summarized in Table 1). Confirming this, we found that co-injection of *Su(H)1* mRNA that lacked the endogenous 5′ and 3′ UTR's, with morpholinos against *Su(H)1* rescued the Su(H)1 phenotype (Table 2); the same effect was seen for a similarly modified Su(H)2 mRNA and morpholinos. Interestingly, co-injection of the *Su(H)1* mRNA with Su(H)2 morpholinos did not effect a rescue, suggesting that there is not a simple biochemical redundancy between the two genes during somitogenesis (Table 2).

Table 2
Summary of rescue experiments

Treatment	Anterior defects (%)	Posterior defects (%)	Total no. of embryos
Su(H)1 MO+mRNA SuH1	0	20	50
Su(H)1 MO+mRNA Su(H)2	0	70	60
Su(H)2 MOs+mRNA Su(H)2	10	10	50
Su(H)2 MOs+mRNA Su(H)1	80	80	55

Total numbers of embryos refers to the total number presumed to be injected that survive until 24 hpf.

Down-regulating either Su(H) gene causes asymmetries in cyclic gene expression

During development, cyclic waves of gene expression are observed as distinct stripes of mRNA that move in a coordinated, bilaterally symmetrical fashion from the posterior to the anterior presomitic mesoderm. In zebrafish these stripes can be observed from tailbud stage to the end of somitogenesis for the genes *her1*, *her7* and *deltaC* (*dlc*) (Henry et al., 2002; Holley et al., 2000; Jiang et al., 2000; Oates and Ho, 2002; Sawada et al., 2000). Data from previous studies suggests that the position at which these oscillations arrest in the anterior PSM by interaction with the determination front dictates the site of the next somitic boundary (Sawada et al., 2001).

When we examined the pattern of mRNA expression of these three genes in the morpholino-injected embryos we found that *Su(H)1* MO injected embryos displayed no defects in any of the cyclic genes at tailbud stage (Fig. 5B), but strikingly, when examined at the 15 somite stage 70% of the embryos showed asymmetries in all three cyclic genes (Fig. 5F). In contrast, the *Su(H)2* morpholino injected embryos already exhibited asymmetries in expression of all of the cyclic genes from tailbud

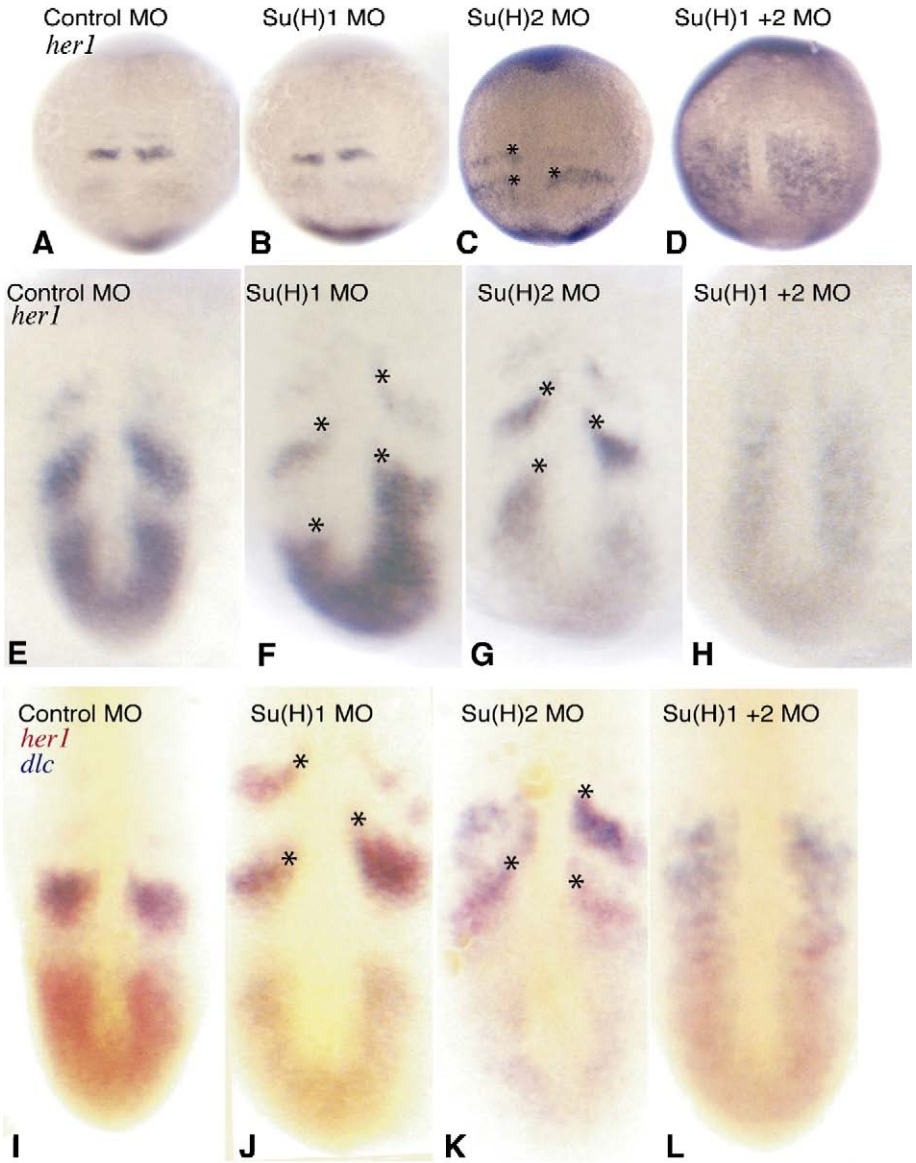

Fig. 5. Left/right asymmetric expression of cyclic genes after *Su(H)* knockdown. (A–D) Expression of the cyclic gene *her1* in the PSM of whole mount bud stage embryos. (A) Control MO-injected embryo ($n=40$) and (B) Su(H)1 MO-injected embryo both display characteristic symmetric stripes of *her1* (100%, $n=50$). (C) Su(H)2 MO-injected embryo: *her1* stripes are left/right (L/R) asymmetric across the midline (75%, $n=55$). (D) Combined Su(H)1 and Su(H)2 MO-injected embryo: cyclic stripes are completely disrupted (80%, $n=60$). (E–H) *her1* expression at 15 somite stage in flat-mounted PSM. (E) Control MO-injected embryo: symmetrical waves of *her1* in the PSM (100%, $n=30$). (F, G) Su(H1) or Su(H)2 MO-injected embryo: the cyclic stripes of *her1* are L/R asymmetric in both anterior and posterior PSM (70%, $n=60$ for each MO). (H) Combined Su(H)1 and Su(H)2 MO-injected embryo: cyclic stripes are disrupted in the PSM (80%, $n=60$). Equivalent results are seen for *her7* and *dlc* gene expression. (I–L) Double in situ hybridization detecting *her1* (red) and *dlc* (blue): the cyclic genes are co-expressed (oscillating in phase) in control MO-injected embryos (I). Despite L/R asymmetric distribution of stripes in Su(H)1 or Su(H)2 MO-injected embryos, *her1* and *dlc* are still co-expressed (85%, $n=50$). (L) Scattered distribution of *her1* and *dlc* expressing cells in combined Su(H)1 and Su(H)2 MO-injected embryo.

stage (Fig. 5C), persisting up to the 15 somite stage (Fig. 5G). Thus, the developmental emergence of the asymmetries in cyclic gene expression patterns is in good agreement with the timing of morphological somite abnormalities for each of the *Su(H)* gene knockdowns.

To control for potential non-specific effects due to asymmetric developmental delay, a control morpholino was injected, but no asymmetries in cyclic gene expression were observed (Figs. 5A,E,I). As a further control for defects caused by potential asymmetric distribution of the *Su(H)* targeted morpholinos, a fluorescently tagged control morpholino was co-injected with the *Su(H)* morpholinos, but no asymmetries in distribution of fluorescence could be observed (Supplementary data, Figure S2). Thus, the observed asymmetries in cyclic gene expression are a result of the specific knockdown of the *Su(H)* genes.

We noted two important hallmarks of asymmetry when comparing left and right sides in these affected embryos: the A/P position of stripes, and the intensity of expression at a given position in the PSM. No systematic L/R bias of the asymmetric waves of gene expression was observed in any clutch of single morpholino injected embryos. Furthermore, when the expression of two cyclic genes was examined together in morpholino-injected embryos, we found that the cyclic genes were co-expressed even when asymmetric (Figs. 5I–L). These data are consistent with a simple, unbiased loss of bilateral symmetry coordination between left and right sides, but with a segmentation oscillator that is nevertheless still periodic. In contrast to single *Su(H)* gene knockdown, when both *Su(H)1* and *Su(H)2* were targeted by specific morpholino co-injection, complete loss of cyclic waves was observed from tailbud stage for all cyclic genes (Figs. 5D,H). This observation is similar to the results of Sieger et al. (2003), consistent with a cross-silencing activity of the previously reported *Su(H)* ORF morpholino.

Su(H) function is required for expression of the retinoic acid catabolizing enzyme-encoding gene cyp26a1, in the tailbud

It is possible that the asymmetries in cyclic gene expression observed after knockdown of a single *Su(H)* gene's function are caused entirely by perturbations to the mechanism of the oscillator itself. Alternatively, reduction of *Su(H)* function might disturb some aspect of the wavefront in the tailbud and PSM that in turn regulates the oscillatory mechanism. Fgf8 and RA have been previously identified as key molecules that create opposing gradients in the embryo that ultimately control the position in the anterior PSM, the determination front, at which the oscillations of the waves of cyclic genes arrest and the new somite boundary is formed (Diez del Corral et al., 2003; Dubrulle et al., 2001; Dubrulle and Pourquie, 2004b; Sawada et al., 2001). In addition, RA has been implicated in the control of bilateral symmetry of cyclic gene expression (Kawakami et al., 2005; Sirbu and Duester, 2006; Vermot et al., 2005; Vermot and Pourquie, 2005). We therefore looked in *Su(H)* morpholino injected embryos between bud and 15 somite stage for effects on the expression of *fgf8* (Reifers et al., 1998) and *raldh2* (Grandel et al., 2002) but no significant differences could be observed (data not shown), indicating that the sources of the Fgf8 and RA entering the PSM were unlikely to be disrupted. We next examined the expression of the *cyp26a1* gene, which codes for the enzymatic activity that creates the degradative sink for RA in the posterior part of the PSM and the tailbud (Abu-Abed et al., 2001; Dobbs-McAuliffe et al., 2004; Emoto et al., 2005; Grandel et al., 2002; Kudoh et al., 2002; Sakai et al., 2001) (Fig. 6A). At the one somite stage, embryos injected with morpholinos to either or both *Su(H)* genes appeared to express normal levels of *cyp26a1* mRNA (data not shown). Strikingly, at the 15 somite stage we found that when morpholinos against either *Su(H)* gene were injected, the levels of *cyp26a1* were attenuated (Figs. 6B,C), and when both Su(H) genes were down-regulated, *cyp26a1* expression was barely detectable (Fig. 6D). In contrast, when mRNA coding for an activated form of Su(H) was injected into the early embryo, posterior expression of *cyp26a1* was up-regulated at 15 somites (Fig. 6E), indicating that *cyp26a1* expression is controlled by Su(H) activity in the tailbud. This data suggests that Su(H) proteins play an essential role in the maintenance, but not the induction of *cyp26a1* expression. Thus, the later appearance of the asymmetric cyclic expression defects in the posterior trunk due to loss of *Su(H)1* knockdown are well correlated with the loss of

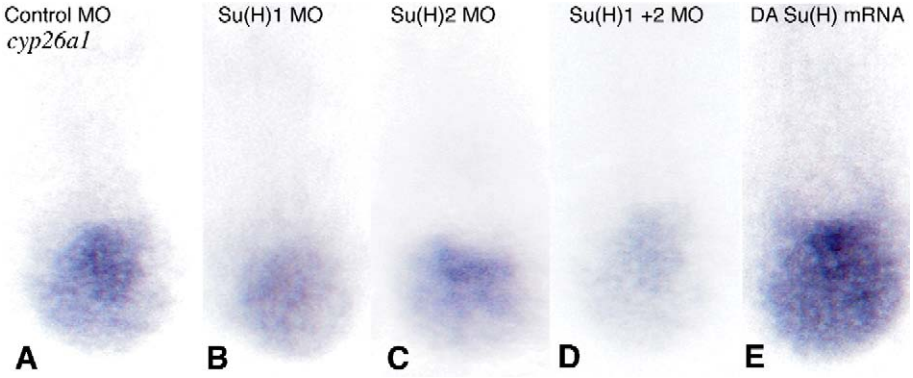

Fig. 6. *Su(H)* activity regulates *cyp26a1* mRNA expression. (A–E) *cyp26a1* expression in 15 somite stage embryos, dorsal views of flat-mounted PSM. (A) Control MO-injected embryo: *cyp26a1* is expressed in tailbud and posterior PSM ($n=50$). (B, C) *cyp26a1* expression domain is reduced in Su(H)1 or Su(H)2 MO-injected embryos (80%, $n=60$ for each MO). (D) Combined Su(H)1 and Su(H)2 MO-injected embryo: *cyp26a1* transcript is barely detectable (85%, $n=65$). (E) Embryos injected with Dominant Activated (DA)-Su(H) mRNA: *cyp26a1* levels are highly increased (80%, $n=50$).

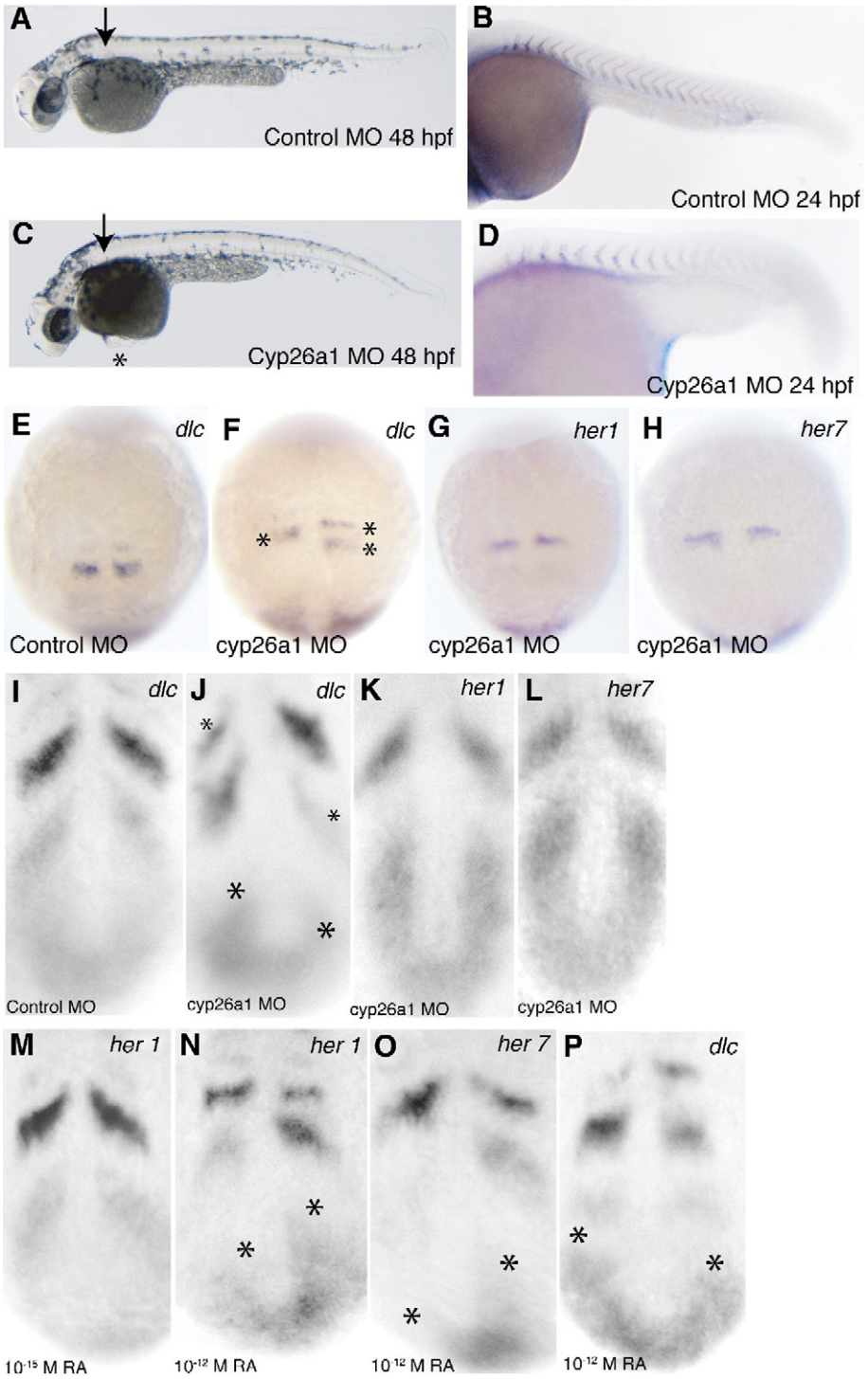

Fig. 7. Knockdown of *cyp26a1* or exogenous RA causes L/R asymmetric cyclic gene expression. (A, C) Lateral views of live 48 hpf embryos. (A) Control MO-injected embryo ($n=40$). (C) *cyp26a1* morphant embryo has smaller eyes and bent body axis; arrow indicates the position of the pectoral fin bud that is reduced in the morphant, asterisk indicates blood pooling on the yolk that occurs only in the morphant embryo (55%, $n=65$). (B, D) Lateral view of myotome boundaries marked by *titin* expression in 24 hpf embryos. (B) Control MO-injected embryo has perfectly symmetrical chevron shaped boundaries along the axis ($n=35$). (D) *cyp26a1* morphant embryo shows smaller abnormally shaped boundaries in the trunk, boundary formation is disrupted more posteriorly associated with abnormal tail shape, higher magnification image than panel B (48%, $n=55$). (E–H) Cyclic gene expression at 2 somite stage in whole mount embryos. In comparison to control-MO injected embryos (E) ($n=32$), *dlc* expression is L/R asymmetric in the *cyp26a1* morphant embryo (asterisks, F) (45% $n=40$). In contrast, *her1* and *her7* expression is L/R symmetrical in the *cyp26a1* morphant (G, H) (100% $n=45$). (I–L) Cyclic gene expression at the 10 somite stage in flat-mounted PSM. *dlc expression* is L/R asymmetric in the *cyp26a1* morphant (asterisks, J) (52% $n=35$) when compared to the control MO-injected embryo (I) ($n=30$), but the L/R symmetry of *her1* and *her7* expression is not affected (K, L) (100% $n=30$). (M, N) *her1* expression at 10 somite stage in flat-mounted PSM. (M) Embryo incubated with 10^{-15} M RA: *her1* expression stripes are L/R symmetric (100%, $n=40$). (N–P) Incubation with 10^{-12} M RA causes L/R asymmetries in the anterior and posterior stripes of *her1*, *her7* and *dlc* expression as indicated by the asterisks (90%, $n=60$).

cyp26a1 expression at 15 somites, but those due to *Su(H)2* knockdown in the anterior trunk are not (see Discussion).

Retinoic acid catabolism is required for L/R symmetric cyclic gene expression

The retinoic acid metabolizing enzyme Cyp26a1 has previously been described as essential for determining territories of hindbrain and spinal cord in zebrafish (Emoto et al., 2005). The *cyp26a1* mutant *giraffe* displays multiple morphological defects, including smaller eyes, a characteristic shorter, curved tail, blood pooling on the yolk and reduced pectoral fin buds, which are phenocopied by a *cyp26a1* morpholino, but the process of segmentation has not been examined (Emoto et al., 2005). If the reduction of *cyp26a1* expression were important in the genesis of the *Su(H)* posterior trunk defects, we would expect a reduction of Cyp26a1 function to recapitulate aspects of the Su(H) phenotype. We therefore investigated whether *cyp26a1* morpholino knockdown would alter the formation of segmental boundaries and importantly, whether any L/R asymmetries in cyclic gene expression could be observed. Injection of a *cyp26a1*-targeted morpholino caused the characteristic morphological defects described previously by Emoto et al. (2005) (Figs. 7A,C). The morphant embryos were examined for defects in boundary formation at 24 hpf and were found to have shorter, broken myotome boundaries and slightly curved, U-shaped boundaries in the anterior trunk; more posteriorly, aberrant tail formation was accompanied by a loss of observable myotome boundaries (Fig. 7D). Expression of the cyclic genes was analysed at 2 somite (Figs. 7E–H) and 10 somite (Figs. 7I–L) stages and *dlc* expression stripes were found to be L/R asymmetric in 45% of embryos ($n=40$) at both stages in the *cyp26a1* morphant embryos (Figs. 7F,J). Surprisingly, normal L/R symmetric waves of gene expression of both *her1* and *her7* were seen in the morphants (Figs. 7G,H,K,L), suggesting that the oscillations of the *dlc* and *her* waves can be uncoupled. These results indicate that a reduction in *cyp26a1* function is likely to contribute to the L/R asymmetry of *dlc* cyclic gene expression observed in the posterior trunk of *Su(H)1* and *Su(H)2* morphant embryos.

A reduction of *cyp26a1* activity in the caudal PSM would be predicted to raise the effective level of RA in this tissue (Emoto et al., 2005; Niederreither et al., 2002). To test whether elevated levels of RA are themselves sufficient to produce cyclic expression asymmetries, wild type embryos were bathed in exogenous RA at a range of low concentrations (10^{-9}–10^{-15} M), and examined for asymmetries in cyclic gene expression. By comparison, exogenous RA concentrations previously shown to affect CNS patterning and the development of cranial ganglia and pectoral fin buds ranged from 10^{-7} to 10^{-9} M (Grandel et al., 2002; Hill et al., 1995; Holder and Hill, 1991). At the lowest concentrations tested (10^{-15} M), cyclic expression patterns were normal (Fig. 7M), but at higher levels (10^{-12} M) we observed L/R asymmetry in *her1*, *her7* and *dlc* cyclic expression domains throughout the tailbud and PSM (Figs. 7N–P). These results indicate that a slightly elevated RA level in the tailbud and PSM is sufficient to generate L/R asymmetries in cyclic expression. Combined with our observations of the *cyp26a1* phenotype, these experiments suggest that the cyclic asymmetries in the posterior trunk in single *Su(H)* gene knockdown embryos may result from an elevation of RA in the tailbud following from a loss of Cyp26a1 catabolic activity.

Discussion

Some embryonic structures must develop with a left/right (L/R) asymmetry, for example organs of the viscera such as heart and liver, whereas others must be symmetrical, such as the somites. Notch and RA signalling have both been implicated in these processes, but the nexus of interaction remains unclear. In this study we have analysed the function of two duplicated *Suppressor of Hairless* (*Su(H)*) genes during early zebrafish development, focusing on their roles in somitogenesis. We report that an apparent evolutionary subdivision of *Su(H)* gene function results in distinct knockdown phenotypes in multiple organ systems, each of which could be viewed as a partial and overlapping *Notch* loss of function. *Su(H)2* is the first gene described with an anterior somite phenotype caused by defective segmentation oscillator function. We also show that the zebrafish *Su(H)* genes are the first Notch signalling components required for bilateral symmetry of both cyclic gene expression and somite morphology. Surprisingly, *Su(H)* function is required for expression of the RA catabolizing enzyme *cyp26a1* in the tailbud, suggesting that an increase in RA levels in the PSM might underlie the cyclic expression asymmetries. Consistent with this notion, a reduction of *cyp26a1* function and low levels of exogenously supplied RA desynchronize the left and right halves of the PSM. Thus, this work is the first evidence that Notch signalling, through Su(H), may have an unexpected role upstream of RA-dependent mechanisms that are thought to generate both the determination front, and to buffer L/R asymmetrical signalling cues.

Two functional Su(H) genes in the zebrafish

Previous studies on Notch signalling have led to a model in which a single, DNA-bound Su(H) protein is responsible for integrating transcriptional responses downstream of diverse Delta and Notch ligands and receptors (reviewed in Bray and Furriols, 2001). However, in contrast to *Drosophila*, nematodes, mice and humans, in which only one *Su(H)* gene has been described (Kawaichi et al., 1992; Zhang et al., 1994), we now show that zebrafish have at least two active *Su(H)* genes. Although zebrafish *Delta* and *Notch* genes show highly restricted and dynamic expression (Appel and Eisen, 1998b; Dornseifer et al., 1997; Haddon et al., 1998; Westin and Lardelli, 1997), ubiquitous distribution of transcript from the two zebrafish *Su(H)* homologs does not yield any clues as to distinct roles in early development. Nevertheless, reduction of the levels of each gene's function using antisense morpholinos resulted in distinct phenotypes during somitogenesis, indicating individual roles for the *Su(H)* homologs in this process. Down-regulation of *Su(H)1* resulted in defects in somite boundary

formation in the posterior trunk, and general defects in tail outgrowth. From about 10 somites onwards, cyclic expression of *her1*, *her7* and *dlc* became asymmetric on either side of the midline, in good agreement with the developmental stage of the somite boundary phenotype onset. In contrast, knockdown of the *Su(H)2* gene causes defects in boundary formation and symmetry starting in the anterior trunk, and asymmetries in cyclic gene expression waves are seen from tailbud stage onwards. Thus, the *Su(H)2* knockdown is the first described phenotype in which anterior somite defects are underlain by specific misregulation of the segmentation oscillator. In each of the single *Su(H)* gene knockdown conditions, the waves of each cyclic gene are still locally coordinated on one side, even though they are out of phase with the contralateral side. These patterns suggest a global problem with the bilateral synchronization of waves throughout the PSM, and not a local problem concerning the synchronization of neighboring cells, as has been previously proposed for a strong loss of Delta/Notch signalling (Jiang et al., 2000).

If both *Su(H)* genes are knocked down, either by co-injection of *Su(H)1* and *Su(H)2* specific morpholinos, or by injection of a morpholino that simultaneously targets both transcripts due to their sequence identity near the start codons (ORF-MO; Sieger et al., 2003), we observe a complete loss of cyclic expression patterns preceding the formation of the first somite, and persisting throughout segmentation stages. This pattern resembles the simultaneous loss of multiple Notch pathway members (Henry et al., 2002; Oates and Ho, 2002; Oates et al., 2005), previously described as a complete failure of the segmentation oscillator. There is therefore some redundancy between the *Su(H)* genes in patterning the anterior trunk, but our observation that *Su(H)1* mRNA cannot rescue the *Su(H)2* knockdown, suggests that this redundancy is not a simple matter of levels of biochemical activity. The zebrafish Su(H) paralogs exhibit almost complete identity throughout their DNA, Notch ICD-ANK, -RAM, and MAM binding domains (Kovall and Hendrickson, 2004; Nam et al., 2006; Wilson and Kovall, 2006), as well as residues involved in binding the CIR and SMRT co-repressors (Fuchs et al., 2001; Hsieh et al., 1999), implying that their interactions with the canonical Notch signalling pathway should be very similar. However, two amino acid changes in a MAM interface in Su(H)2 relative to Su(H)1 and other vertebrate peptides suggests that the zebrafish Su(H) proteins may differ in their selectivity for members of the MAM family of essential co-activators (Wu and Griffin, 2004). Most strikingly, a high amino acid divergence is found in the C-terminal tail, a region that has not been previously ascribed a distinct function or included in crystals. Given the immediate proximity of the Su(H) tail to the N-terminus of the NICD ANK repeats in crystal structures, we speculate that it could interact selectively with the relatively unstructured C-terminal 90 amino acids of the RAM domain (Wilson and Kovall, 2006) from different Notch receptors. Experiments using these domains to identify interaction partners may help to define their role. Importantly, the development of reagents in this study capable of targeting each *Su(H)* gene individually enabled us to take advantage of the redundancy present in the zebrafish system to reveal novel bilaterally asymmetric cyclic expression pattern defects not previously observed by loss or knockdown of a Notch pathway gene.

Embryonic laterality, Notch and retinoic acid signalling

Targeting of both zebrafish *Su(H)* genes in the early embryo leads to a randomization in the positioning of the heart, suggesting a role for *Su(H)* function in left–right patterning of the viscera of the embryo. This is consistent with recent evidence that Notch signalling is required for visceral L/R asymmetry in zebrafish, chicks and mice, although it is not the earliest, symmetry-breaking event. In mice, *Dll1*, *RBP-κJ*, and *Notch1*/*Notch2* compound mutants exhibit multiple visceral asymmetry defects (Krebs et al., 2003; Przemeck et al., 2003; Raya et al., 2003). Could the asymmetries in cyclic gene expression and somite boundary placement we observed follow from an early perturbation in Notch determined left–right laterality? Arguing against this proposition is the observation that although early pharmacological blockade of γ-secretase cleavage of the Notch intracellular domain during epiboly causes visceral asymmetries, later treatment during segmentation stages instead causes somitic defects in embryos with normal situs (Kawakami et al., 2005). This defines an early window of action for Notch signalling in the development of visceral laterality, and a non-overlapping period where Notch signalling is required for somitogenesis. Furthermore, in single *Su(H)* gene knockdown experiments in which the segmentation asymmetries are observed, heart defects are usually the result of an arrest of cardiac development at the tube elongation stage, and not a perturbation of situs. We therefore favor an interpretation in which there are multiple independent effects of *Su(H)* knockdown resulting from distinct spatial and temporal requirements for *Su(H)1* and *Su(H)2* functions. To date the only other gene that has been shown to affect both left/right visceral symmetry and symmetry of the somites is a *doublesex* related gene, *terra* (Saude et al., 2005). The relationship between *terra* and the *Su(H)* genes is unknown; the possibility remains that they may be acting together to control laterality in the developing embryo.

Retinoic acid and segmentation—up- or downstream?

In current clock and wavefront or gradient models for vertebrate somitogenesis, control of the arrest of oscillations by FGF and RA gradients in the PSM is critical for determining the size of the newly forming segment (Aulehla and Herrmann, 2004; Dubrulle and Pourquie, 2004a). RA appears to play an important role in modulating the response of the PSM cells to their local level of FGF. RA synthesis is completed in the already formed somites by the Raldh2 enzyme, and catabolized by *cyp26a1* in the tailbud, generating a gradient of RA and RA-responsive transgenes, across the PSM (Sirbu and Duester, 2006; Vermot et al., 2005). Reduction of RA levels in quail, mouse and *Xenopus* has been shown to change the response of PSM cells to FGF signalling, and thereby increase the size of the PSM while decreasing the size of the forming somites (Diez del

Corral et al., 2003; Moreno et al., 2004; Sirbu and Duester, 2006). Thus, changes in the gradient of either FGF signalling or RA concentration would be predicted to alter somite size, and unilateral perturbations would be needed to generate asymmetry.

A second role for RA in somitogenesis was revealed by experiments showing that elimination of RA synthesis disturbs the L/R symmetry of forming somites in mouse, chick and zebrafish (Kawakami et al., 2005; Sirbu and Duester, 2006; Vermot et al., 2005; Vermot and Pourquie, 2005). In these experiments, somites on one side of the midline formed in advance of their contralateral counterparts, and this morphological asymmetry was accompanied by marked asymmetries in the cyclic expression patterns throughout the tailbud and PSM. From these findings, RA was proposed to constitute a buffering mechanism to protect the labile segmentation process from left–right laterality signals responsible for asymmetric pattering of the lateral plate visceral organ primordial (Brent, 2005; Hornstein and Tabin, 2005). Thus, both the determination front and the control of symmetry are regulated by RA, but it is not clear if these aspects of somitogenesis are independent mechanisms, or two sides of the same coin. Recently, studies in mice have indicated that RA antagonizes FGF8 expression in the node ectoderm and posterior neural plate, but not the underlying paraxial mesoderm, in contrast to standard determination front models (Sirbu and Duester, 2006; Dubrulle and Pourquie, 2004a). Furthermore, somite asymmetry occurs only after a decrease in somite size in *Raldh2*$^{-/-}$ embryos, suggesting that determination front positioning and symmetry loss are sequential responses of the mesoderm to a loss of RA signalling in the ectoderm (Sirbu and Duester, 2006). Whether these striking results will translate to the zebrafish or other species is a matter for further studies.

In principle there are two explanations for the asymmetry we observed in somite formation and cyclic expression patterns after knockdown of single *Su(H)* genes. Firstly, the asymmetries could be generated entirely within the oscillator itself, perhaps by modulating cell-to-cell communication via Notch signalling. Recently, evidence of the ability of PSM cells to "phase accelerate" their neighbors through DeltaC has been presented, demonstrating a L/R asymmetrical response of *her1* expression waves to a unilateral clone of *dlc*-overexpressing cells (Horikawa et al., 2006). However, our demonstration of even, bilateral distribution of Su(H) MOs in affected embryos (Supplementary Figure S2), makes this specific mechanism seem unlikely.

Alternatively, by changing RA catabolism in the tailbud through a reduction in *cyp26a1* expression, in turn caused by loss of Su(H)-dependent maintenance, it seems likely we may be observing effects on cyclic gene expression downstream of changes to the determination front or related RA-dependent laterality buffering mechanism. Consistent with an important contribution of tailbud *cyp26a1* expression to the posterior *Su(H)* phenotype, loss of *cyp261a* in fish and mice leads to tail defects, and in mice axial skeletal abnormalities including fusion and bifurcations of ribs and vertebral bodies (Emoto et al., 2005; Sakai et al., 2001). The striking L/R asymmetries in *dlc* expression we observed throughout segmentation stages in *cyp26a1* morphant embryos is direct functional evidence of the necessity of *cyp26a1* for the L/R symmetrical expression of cyclic genes. We have also shown that exogenously supplied RA produces bilateral asymmetry in cyclic gene expression waves, indicating that elevated RA is sufficient to desynchronize oscillations in the left and right sides of the PSM. Importantly, these asymmetries, like those of the *Su(H)* knockdowns, are visible in the tailbud and caudal PSM, indicating that the defect occurs early in the propagation of a cyclic expression wave in the most immature paraxial mesoderm. Combined with previous results showing asymmetric cyclic gene expression following loss of RA production in zebrafish (Kawakami et al., 2005), these findings indicate that too much or too little RA in the PSM disrupts the bilateral coordination of cyclic gene expression waves.

Comparison of our asymmetrical phenotypes to those reported due to loss of RA production (Kawakami et al., 2005; Vermot et al., 2005; Vermot and Pourquie, 2005) reveals two important differences: first, RA deficiency leads to a reproducible handedness to the asymmetry defects; whereas the Su(H) knockdowns do not. Instead, in this respect they resemble more closely perturbations of other steps in the laterality pathway in zebrafish, such as inhibition of H+/K+-ATP transporter, translation of left–right dynein, or γ-secretase cleavage that lead to unbiased asymmetries in somite formation (Kawakami et al., 2005), although it is important to note that cyclic gene expression was not assayed in these cases. Second, the bilateral asymmetry observed in RA deficiency was restricted to a developmental window between approximately somites 6 and 14, in all species examined (Kawakami et al., 2005; Vermot et al., 2005; Vermot and Pourquie, 2005), whereas for *Su(H)2* knockdown no temporal restriction was observed in cyclic gene expression asymmetries, and somites 1 to 8 were the most sensitive to morphological perturbation. These differences in phenotype may simply be due to the difference between gain or loss of RA functions, but at present we cannot rule out a direct contribution from perturbation of the segmentation oscillator, or other Su(H) target genes, in addition. In this light, it is worth noting that Su(H) proteins may act as transcriptional repressors in the absence of Notch activation (Bray and Furriols, 2001), and aspects of their loss of function phenotypes may result from inappropriate activation of normally repressed target genes.

One outstanding question is why the Su(H)2 MO causes asymmetrical cyclic expression domains at early somitogenesis stages, even though expression levels of *cyp26a1* appear unchanged. Although *cyp26b1* and *cyp26c1* are not expressed in the tailbud at these stages (Gu et al., 2005; Zhao et al., 2005), the possibility of other Cyp26-related activities remains. Indeed, since RA signalling is regulated by different mechanisms at different developmental stages, other proteins involved in RA signalling such as the retinoic acid receptors (RAR and RXR families; Mark et al., 2006) might be controlled by *Su(H)2* in the early tailbud. Nonetheless, since *dlc* expression asymmetries are seen at early somite stages due to *cyp26a1* reduction of function, it may be that Cyp26a1

activity is in fact reduced in the early tailbud in the *Su(H)2* knockdown animals, and the embryo is a better sensor than our in situ detection methods.

The striking observation that *dlc* expression becomes asymmetric after *cyp26a1* morpholino knockdown, while that of *her1* and *her7* does not indicate that the oscillations of these genes can be uncoupled. It is possible that transcription of *dlc* is more sensitive to RA levels than the *Her* genes, and that the *cyp26a1* knockdown increases the level of RA in the tailbud sufficiently to affect *dlc*, but not *her1* and *her7*, whereas exogenously added RA levels are enough to affect all three genes. Perturbations that uncouple the dynamic expression of cyclic genes from each other have been previously noted. Inhibition of protein synthesis by cycloheximide affects *Lfng* expression but not that of *c-Hairy1* in the chick (McGrew et al., 1998), while *Axin2* and *Snail1* retain dynamic expression in *Dll1* or *Hes7* mouse mutants, in which *Lfng* expression is no longer cyclic (Aulehla et al., 2003; Dale et al., 2006). These latter cases are thought to provide evidence for distinct Notch and Wnt-based oscillators, which are coupled in wildtype embryos, potentially leading to a higher precision of the overall oscillatory output. Strikingly, over-expression of *Axin2* in the mouse PSM leads to L/R asynchrony of cyclic *Lfng* stripes (Aulehla et al., 2003), suggesting that interfering with Wnt–Notch coupling may interfere also with segmental symmetry. In the zebrafish, there are currently no reports of a role for Wnt signaling in segmentation, and therefore further experiments will be necessary to explain the decoupling of *dlc* from the *her* genes seen in our experiments.

Regardless of the exact molecular mechanisms, our results clearly indicate that *Su(H)*, previously known as a component of the segmentation oscillator, plays an additional role in the tailbud upstream of RA metabolism. Our results therefore suggest a modification of the oscillator and determination front model. We hypothesize that Su(H), downstream of Delta/Notch signalling, appears to perform a dual role in the tailbud: firstly, it is required for synchronization and maintenance of the cyclic gene oscillations of the segmentation clock, and secondly it is required to maintain the catabolic sink for RA in the posterior of the elongating animal, thereby potentially modulating the position of the determination front, and/or allowing RA asymmetry buffering to occur correctly. We speculate that the tailbud maintains its capacity as an RA sink in response to the ongoing Notch signalling that originates in the segmentation oscillator.

Acknowledgments

We would like to thank S. Abdelilah for sending plasmid reagents, M. Brand and L. Rohde for comments on the manuscript, the fish facility staff of the MPI-CBG, and R. Ho, in whose lab this work was started.

Appendix A. Supplementary data

Supplementary data associated with this article can be found, in the online version, at doi:10.1016/j.ydbio.2006.10.003.

References

Abu-Abed, S., Dolle, P., Metzger, D., Beckett, B., Chambon, P., Petkovich, M., 2001. The retinoic acid-metabolizing enzyme, CYP26A1, is essential for normal hindbrain patterning, vertebral identity, and development of posterior structures. Genes Dev. 15, 226–240.

Appel, B., Eisen, J., 1998a. Regulation of neuronal specification in the zebrafish spinal cord by Delta function. Development 125, 371–380.

Appel, B., Eisen, J.S., 1998b. Regulation of neuronal specification in the zebrafish spinal cord by Delta function. Development 125, 371–380.

Aulehla, A., Herrmann, B.G., 2004. Segmentation in vertebrates: clocks and gradient finally joined. Genes Dev. 18, 2060–2067.

Aulehla, A., Johnson, R.L., 1999. Dynamic expression of lunatic fringe suggests a link between notch signaling and an autonomous cellular oscillator driving somite segmentation. Dev. Biol. 207, 49–61.

Aulehla, A., Wehrle, C., Brand-Saberi, B., Kemler, R., Gossler, A., Kanzler, B., Herrmann, B.G., 2003. Wnt3a plays a major role in the segmentation clock controlling somitogenesis. Dev. Cell 4, 395–406.

Barrantes, I.B., Elia, A.J., Wunsch, K., De Angelis, M.H., Mak, T.W., Rossant, J., Conlon, R.A., Gossler, A., de la Pompa, J.L., 1999. Interaction between Notch signalling and Lunatic fringe during somite boundary formation in the mouse. Curr. Biol. 9, 470–480.

Bessho, Y., Miyoshi, G., Sakata, R., Kageyama, R., 2001a. Hes7: a bHLH-type repressor gene regulated by Notch and expressed in the presomitic mesoderm. Genes Cells 6, 175–185.

Bessho, Y., Sakata, R., Komatsu, S., Shiota, K., Yamada, S., Kageyama, R., 2001b. Dynamic expression and essential functions of Hes7 in somite segmentation. Genes Dev. 15, 2642–2647.

Bessho, Y., Hirata, H., Masamizu, Y., Kageyama, R., 2003. Periodic repression by the bHLH factor Hes7 is an essential mechanism for the somite segmentation clock. Genes Dev.

Bray, S., Furriols, M., 2001. Notch pathway; making sense of suppressor of hairless. Curr. Biol. 11, R217–R221.

Brent, A., 2005. Somite formation: where left meets right. Curr. Biol. 15, R468–R470.

Dale, J.K., Malapert, P., Chal, J., Vilhais-Neto, G., Maroto, M., Johnson, T., Jayasinghe, S., Trainor, P., Herrmann, B.G., Pourquie, O., 2006. Oscillations of the snail genes in the presomitic mesoderm coordinate segmental patterning and morphogenesis in vertebrate somitogenesis. Dev. Cell 3, 355–366.

Diez del Corral, R., Olivera-Martinez, I., Goriely, A., Gale, E., Maden, M., Storey, K., 2003. Opposing FGF and retinoid pathways control ventral neural pattern, neuronal differentiation, and segmentation during body axis extension. Neuron 40, 65–79.

Dobbs-McAuliffe, B., Zhao, Q., Linney, E., 2004. Feedback mechanisms regulate retinoic acid production and degradation in the zebrafish embryo. Mech. Dev. 121, 339–350.

Dornseifer, P., Takke, C., Campos-Ortega, J.A., 1997. Overexpression of a zebrafish homologue of the Drosophila neurogenic gene Delta perturbs differentiation of primary neurons and somite development. Mech. Dev. 63, 159–171.

Dubrulle, J., Pourquie, O., 2002. From head to tail: links between the segmentation clock and antero-posterior patterning of the embryo. Curr. Opin. Genet. Dev. 12, 519–523.

Dubrulle, J., Pourquie, O., 2004a. Coupling segmentation to axis formation. Development 131, 5783–5793.

Dubrulle, J., Pourquie, O., 2004b. fgf8 mRNA decay establishes a gradient that couples axial elongation to patterning in the vertebrate embryo. Nature 427 (6973), 419–422.

Dubrulle, J., McGrew, M.J., Pourquie, O., 2001. FGF signaling controls somite boundary position and regulates segmentation clock control of spatiotemporal Hox gene activation. Cell 106, 219–232.

Dunwoodie, S.L., Clements, M., Sparrow, D.B., Sa, X., Conlon, R.A., Beddington, R.S., 2002. Axial skeletal defects caused by mutation in the spondylocostal dysplasia/pudgy gene Dll3 are associated with disruption of the segmentation clock within the presomitic mesoderm. Development 129, 1795–1806.

Emoto, Y., Wada, H., Okamoto, H., Kudo, A., Imai, Y., 2005. Retinoic acid-

metabolizing enzyme Cyp26a1 is essential for determining territories of hindbrain and spinal cord in zebrafish. Dev. Biol. 278, 415–427.

Evrard, Y.A., Lun, Y., Aulehla, A., Gan, L., Johnson, R.L., 1998. lunatic fringe is an essential mediator of somite segmentation and patterning. Nature 394, 377–381.

Forsberg, H., Crozet, F., Brown, N.A., 1998. Waves of mouse Lunatic fringe expression, in four-hour cycles at two-hour intervals, precede somite boundary formation. Curr. Biol. 8, 1027–1030.

Fuchs, K., Bommer, G., Dumont, E., Christoph, B., Vidal, M., Kremmer, E., Kempkes, B., 2001. Mutational analysis of the J recombination signal sequence binding protein (RBP-J)/Epstein–Barr virus nuclear antigen 2 (EBNA2) and RBP-J/Notch interaction. Eur. J. Biochem. 268, 4639–4646.

Gajewski, M., Sieger, D., Alt, B., Leve, C., Hans, S., Wolff, C., Rohr, K.B., Tautz, D., 2003. Anterior and posterior waves of cyclic her1 gene expression are differentially regulated in the presomitic mesoderm of zebrafish. Development 130, 4269–4278.

Gajewski, Elmasri, H., Girschick, M., sieger, D., Winkler, C., 2006. Comparative analysis of her genes during fish somitogenesis suggests a mouse/chick-like mode of oscillation in medaka. Dev. Genes Evol. 216, 315–332.

Grandel, H., Lun, K., Rauch, G.J., Rhinn, M., Piotrowski, T., Houart, C., Sordino, P., Kuchler, A., Schulte-Merker, S., Geisler, R., Holder, N., Wilson, S., Brand, M., 2002. Retinoic acid signalling in the zebrafish embryo is necessary during pre-segmentation stages to pattern the anterior–posterior axis of the CNS and to induce a pectoral fin bud. Development 129, 2851–2865.

Gu, X., Xu, F., Wang, X., Gao, X., Zhao, Q., 2005. Molecular cloning and expression of a novel CYP26 gene (cyp26d1) during zebrafish early development. Gene Expr. Patterns 6, 733–739.

Haddon, C., Smithers, L., Schneider-Maunoury, S., Coche, T., Henrique, D., Lewis, J., 1998. Multiple delta genes and lateral inhibition in zebrafish primary neurogenesis. Development 125, 359–370.

Henry, C.A., Urban, M.K., Dill, K.K., Merlie, J.P., Page, M.F., Kimmel, C.B., Amacher, S.L., 2002. Two linked hairy/Enhancer of split-related zebrafish genes, her1 and her7, function together to refine alternating somite boundaries. Development 129, 3693–3704.

Hill, J., Clarke, J., Vargesson, N., Jowett, T., Holder, N., 1995. Exogenous retinoic acid causes specific alterations in the development of the midbrain and hindbrain of the zebrafish embryo including positional respecification of the Mauthner neuron. Mech. Dev. 50, 3–6.

Hirata, H., Yoshiura, S., Ohtsuka, T., Bessho, Y., Harada, T., Yoshikawa, K., Kageyama, R., 2002. Oscillatory expression of the bHLH factor Hes1 regulated by a negative feedback loop. Science 298, 840–843.

Holder, N., Hill, J., 1991. Retinoic acid modifies development of the midbrain–hindbrain border and affects cranial ganglion formation in zebrafish embryos. Development 113, 1159–1170.

Holley, S.A., Geisler, R., Nusslein-Volhard, C., 2000. Control of her1 expression during zebrafish somitogenesis by a delta-dependent oscillator and an independent wave-front activity. Genes Dev. 14, 1678–1690.

Holley, S.A., Julich, D., Rauch, G.J., Geisler, R., Nusslein-Volhard, C., 2002. her1 and the notch pathway function within the oscillator mechanism that regulates zebrafish somitogenesis. Development 129, 1175–1183.

Horikawa, K., Ishimatsu, K., Yoshimoto, E., Kondo, S., H, T., 2006. Noise-resistant and synchronized oscillation of the segmentation clock. Nature 441, 719–723.

Hornstein, E., Tabin, C., (2005). Developmental Biology: asymmetrical threat averted.

Hsieh, J., Zhou, S., Chen, L., Young, D., Hayward, S., 1999. CIR, a corepressor linking the DNA binding factor CBF1 to the histone deacetylase complex. Proc. Natl. Acad. Sci. 96, 23–28.

Hukriede, N.A., Joly, L., Tsang, M., Miles, J., Tellis, P., Epstein, J., Barbazuk, W.B., Li, F.N., Paw, B., Postlethwait, J.H., Hudson, T.J., Zon, L.I., McPherson, J.D., Chevrette, M., Dawid, I.B., Johnson, S.L., Ekker, M., 1999. Radiation hybrid mapping of the zebrafish genome. PNAS 10554–10556.

Inoue, A., Takahashi, M., Hatta, K., Hotta, Y., Okamoto, H., 1994. Developmental regulation of islet-1 mRNA expression during neuronal differentiation in embryonic zebrafish. Dev. Dyn. 199, 1–11.

Ishikawa, A., Kitajima, S., Takahashi, Y., Kokubo, H., Kanno, J., Inoue, T., Saga, Y., 2004. Mouse Nkd1, a Wnt antagonist, exhibits oscillatory gene expression in the PSM under the control of Notch signaling. Mech. Dev. 121, 1443–1453.

Itoh, M., Kim, C.H., Palardy, G., Oda, T., Jiang, Y.J., Maust, D., Yeo, S.Y., Lorick, K., Wright, G.J., Ariza-McNaughton, L., Weissman, A.M., Lewis, J., Chandrasekharappa, S.C., Chitnis, A.B., 2003. Mind bomb is a ubiquitin ligase that is essential for efficient activation of Notch signaling by Delta. Dev. Cell 4, 67–82.

Jiang, Y.J., Brand, M., Heisenberg, C.P., Beuchle, D., Furutani-Seiki, M., Kelsh, R.N., Warga, R.M., Granato, M., Haffter, P., Hammerschmidt, M., Kane, D.A., Mullins, M.C., Odenthal, J., van Eeden, F.J., Nusslein-Volhard, C., 1996. Mutations affecting neurogenesis and brain morphology in the zebrafish, *Danio rerio*. Development 123, 205–216.

Jiang, Y.J., Aerne, B.L., Smithers, L., Haddon, C., Ish-Horowicz, D., Lewis, J., 2000. Notch signalling and the synchronization of the somite segmentation clock. Nature 408, 475–479.

Jouve, C., Palmeirim, I., Henrique, D., Beckers, J., Gossler, A., Ish-Horowicz, D., Pourquie, O., 2000. Notch signalling is required for cyclic expression of the hairy-like gene HES1 in the presomitic mesoderm. Development 127, 1421–1429.

Julich, D., Hwee Lim, C., Round, J., Nicolaije, C., Schroeder, J., Davies, A., Geisler, R., Lewis, J., Jiang, Y., Holley, S.A., Consortium, T.S., 2005. beamter/deltaC and the role of Notch ligands in the zebrafish somite segmentation, hindbrain neurogenesis and hypochord differentiation. Dev. Biol. 286, 391–404.

Kawaichi, M., Oka, C., Shibayama, S., Koromilas, A., Matsunami, N., Hamaguchi, Y., Honjo, T., 1992. Genomic organization of mouse J kappa recombination signal binding protein (RBP-J kappa) gene. J. Biol. Chem. 267, 4016–4022.

Kawakami, Y., Raya, A., Raya, R., Rodriguez-Esteban, C., Belmonte, J., 2005. Retinoic acid signalling links left–right asymmetric patterning and bilaterally symmetric somitogenesis in the zebrafish embryo. Nature 435, 165–171.

Kawamura, A., Koshida, S., Hijikata, H., Sakaguchi, T., Kondoh, H., Takada, S., 2005. Zebrafish hairy/enhancer of split protein links FGF signaling to cyclic gene expression in the periodic segmentation of somites. Genes Dev. 1156–1161.

Kimmel, C.B., Ballard, W.W., Kimmel, S.R., Ullmann, B., Schilling, T.F., 1995. Stages of embryonic development of the zebrafish. Dev. Dyn. 203, 253–310.

Koizumi, K., Nakajima, M., Yuasa, S., Saga, Y., Sakai, T., Kuriyama, T., Shirasawa, T., Koseki, H., 2001. The role of presenilin 1 during somite segmentation. Development 128, 1391–1402.

Kovall, R., Hendrickson, W., 2004. Crystal structure of the nuclear effector of Notch signaling, CSL, bound to DNA. EMBO J. 23, 3441–3451.

Krebs, L., Iwai, N., Nonaka, S., Welsh, I., Lan, Y., Jiang, R., Saijoh, Y., O'Brien, T., Hamada, H., Gridley, T., 2003. Notch signaling regulates left–right asymmetry determination by inducing Nodal expression. Genes Dev. 17.

Kudoh, T., Wilson, S., Dawid, I., 2002. Distinct roles for Fgf, Wnt and retinoic acid in posteriorizing the neural ectoderm. Development 129, 4335–4346.

Leimeister, C., Dale, K., Fischer, A., Klamt, B., Hrabe de Angelis, M., Radtke, F., McGrew, M.J., Pourquie, O., Gessler, M., 2000. Oscillating expression of c-Hey2 in the presomitic mesoderm suggests that the segmentation clock may use combinatorial signaling through multiple interacting bHLH factors. Dev. Biol. 227, 91–103.

Leve, C., Gajewski, M., Rohr, K.B., Tautz, D., 2001. Homologues of c-hairy1 (her9) and lunatic fringe in zebrafish are expressed in the developing central nervous system, but not in the presomitic mesoderm. Dev. Genes Evol. 211, 493–500.

Li, Y., Fenger, U., Niehrs, C., Pollet, N., 2003. Cyclic expression of esr9 gene in Xenopus presomitic mesoderm. Differentiation 71, 83–89.

Mark, M., Ghyselinck, N., Chambon, P., 2006. Function of retinoid nuclear receptors: lessons from genetic and pharmacological dissections of the retinoic acid signaling pathway during mouse embryogenesis. Annu. Rev. Pharmacol. Toxicol. 46, 451–480.

Masamizu, Y., Ohtsuka, T., Takashima, Y., Nagahara, H., Takenaka, Y., Yoshikawa, K., Okamura, H., Kageyama, R., 2006. Real-time imaging of the somite segmentation clock: revelation of unstable oscillators in the

individual presomitic mesoderm cells. Proc. Natl. Acad. Sci. 103, 1313–1318.
McGrew, M.J., Dale, J.K., Fraboulet, S., Pourquie, O., 1998. The lunatic fringe gene is a target of the molecular clock linked to somite segmentation in avian embryos. Curr. Biol. 8, 979–982.
Morales, A.V., Yasuda, Y., Ish-Horowicz, D., 2002. Periodic Lunatic fringe expression is controlled during segmentation by a cyclic transcriptional enhancer responsive to notch signaling. Dev. Cell 3, 63–74.
Moreno, T., Kintner, C., 2004. Regulation of segmental patterning by retinoic acid signaling during Xenopus somitogenesis. Dev. Cell 6, 205–218.
Nam, Y., Weng, A., Aster, J., Blacklow, S., 2003. Structural requirements for assembly of the CSL–intracellular Notch1–Mastermind-like 1 transcriptional activation complex. J. Biol. Chem. 278, 2132–2139.
Nam, Y., Sliz, P., Song, L., Aster, J., Blacklow, S., 2006. Structural basis for cooperativity in recruitment of MAML coactivators to Notch transcription complexes. Cell 124, 973–983.
Niederreither, K., Vermot, J., Fraulob, V., Chambon, P., Dolle, P., 2002. Retinaldehyde dehydrogenase 2 (RALDH2) independent patterns of retinoic acid synthesis in the mouse embryo. Proc. Natl. Acad. Sci. 99, 16111–16116.
Oates, A.C., Ho, R.K., 2002. Hairy/E(spl)-related (Her) genes are central components of the segmentation oscillator and display redundancy with the Delta/Notch signaling pathway in the formation of anterior segmental boundaries in the zebrafish. Development 129, 2929–2946.
Oates, A.C., Mueller, C., Ho, R.K., 2005. Cooperative function of deltaC and her7 in anterior segment formation. Dev. Biol. 280, 133–149.
Palmeirim, I., Henrique, D., Ish-Horowicz, D., Pourquie, O., 1997. Avian hairy gene expression identifies a molecular clock linked to vertebrate segmentation and somitogenesis. Cell 91, 639–648.
Palmeirim, I., Dubrulle, J., Henrique, D., Ish-Horowicz, D., Pourquie, O., 1998. Uncoupling segmentation and somitogenesis in the chick presomitic mesoderm. Dev. Genet. 23, 77–85.
Pourquie, O., 2001. Vertebrate somitogenesis. Annu. Rev. Cell Dev. Biol. 17, 311–350.
Pourquie, O., Kusumi, K., 2001. When body segmentation goes wrong. Clin. Genet. 60, 409–416.
Pourquie, O., Tam, P.P., 2001. A nomenclature for prospective somites and phases of cyclic gene expression in the presomitic mesoderm. Dev. Cell 1, 619–620.
Prince, V.E., Joly, L., Ekker, M., Ho, R.K., 1998. Zebrafish hox genes: genomic organization and modified colinear expression patterns in the trunk. Development 125, 407–420.
Prince, V.E., Holley, S.A., Bally-Cuif, L., Prabhakaran, B., Oates, A.C., Ho, R.K., Vogt, T.F., 2001. Zebrafish lunatic fringe demarcates segmental boundaries. Mech. Dev. 105, 175–180.
Przemeck, G., Heinzmann, U., Beckers, J., Hrabe de Angelis, M., 2003. Node and midline defects are associated with left–right development in Delta1 mutant embryos. Development 130, 3–13.
Raya, A., Kawakami, Y., Rodriguez-Esteban, C., Buscher, D., Koth, C., Itoh, T., Morita, M., Raya, R., Dubova, I., Bessa, J., de la Pompa, J.L., Belmonte, J., 2003. Notch activity induces Nodal expression and mediates the establishment of left–right asymmetry in vertebrate embryos. Genes Dev. 17, 1213–1218.
Reifers, F., Bohli, H., Walsh, E., Crossley, P., Stainier, D., Brand, M., 1998. Fgf8 is mutated in zebrafish acerebellar(ace) mutants and is required for maintenance of midbrain–hindbrain boundary development and somitogenesis. Development 125, 2381–2395.
Sakai, T., Taniguchi, Y., Tamura, K., Minoguchi, S., Fukuhara, T., Strobl, L., Zimber-Strobl, U., Bornkamm, G., Honjo, T., 1998. Functional replacement of the intracellular region of the Notch1 receptor by Epstein–Barr virus nuclear antigen 2. J. Virol. 72, 6034–6039.
Sakai, Y., Meno, C., Fujii, H., Nishino, J., Shiratori, H., Saijoh, Y., Rossant, J., Hamada, H., 2001. The retinoic acid-inactivating enzyme CYP26 is essential for establishing an uneven distribution of retinoic acid along the anterio-posterior axis within the mouse embryo. Genes Dev. 15, 213–225.
Saude, L., Lourenco, R., Goncalves, A., Palmeirim, I., 2005. terra is a left–right asymmetry gene required for left–right synchronization of the segmentation clock. Nat. Cell Biol. 918–920.
Sawada, A., Fritz, A., Jiang, Y., Yamamoto, A., Yamasu, K., Kuroiwa, A., Saga, Y., Takeda, H., 2000. Zebrafish Mesp family genes, mesp-a and mesp-b are segmentally expressed in the presomitic mesoderm, and Mesp-b confers the anterior identity to the developing somites. Development 127, 1691–1702.
Sawada, A., Shinya, M., Jiang, Y.J., Kawakami, A., Kuroiwa, A., Takeda, H., 2001. Fgf/MAPK signalling is a crucial positional cue in somite boundary formation. Development 128, 4873–4880.
Schweisguth, F., 2004. Notch signaling activity. Curr. Biol. 14, R129–R138.
Sieger, D., Tautz, D., Gajewski, M., 2003. The role of Suppressor of Hairless in Notch mediated signalling during zebrafish somitogenesis. Mech. Dev. 129 (9), 1083–1094.
Sieger, D., Tautz, D., Gajewski, M., 2004. her11 is involved in the somitogenesis clock in zebrafish. Dev. Genes Evol. 214, 393–406.
Sirbu, I., Duester, G., 2006. Retinoic-acid signalling in node ectoderm and posterior neural plate directs left–right patterning of somitic mesoderm. Nat. Cell Biol. 271–277.
Thompson, J., Higgins, D., Gibson, T., 1994. CLUSTAL W: improving the sensitivity of progressive multiple sequence alignment through sequence weighting, position-specific gap penalties and weight matrix choice. Nucleic Acid Res. 22, 4673–4680.
van Eeden, F.J., Granato, M., Schach, U., Brand, M., Furutani-Seiki, M., Haffter, P., Hammerschmidt, M., Heisenberg, C.P., Jiang, Y.J., Kane, D.A., Kelsh, R.N., Mullins, M.C., Odenthal, U., Warga, R.M, Allende, M.L., Weinberg, E.S., Nusslein-Volhard, C., 1996. Mutations affecting somite formation and patterning in the zebrafish, *Danio rerio*. Development 123, 153–164.
Vermot, J., Pourquie, O., 2005. Retinoic acid coordinates somitogenesis and left–right patterning in vertebrate embryos. Nature 435, 215–220.
Vermot, J., Gallego Llamas, J., Fraulob, V., Niederreither, K., Chambon, P., Dolle, P., 2005. Retinoic acid controls bilateral symmetry of somite formation in the mouse embryo. Science 308, 563–566.
Westin, J., Lardelli, M., 1997. Three novel Notch genes in zebrafish: implications for vertebrate Notch gene evolution and function. Dev. Genes Evol. 207, 51–63.
Wilson, J., Kovall, R., 2006. Crystal structure of the CSL–Notch–Mastermind ternary complex bound to DNA. Cell 124, 985–996.
Wu, L., Griffin, J., 2004. Modulation of Notch signaling by mastermind-like (MAML) transcriptional co-activators and their involvement in tumorigenesis. Semin. Cancer Biol. 14, 348–356.
Zhang, N., Gridley, T., 1998. Defects in somite formation in lunatic fringe-deficient mice. Nature 394, 374–377.
Zhang, M., Tang, X., Jin, C., Logeat, F., Alain, I., Kondo, S., Sun, K., Yokoyama, K., 1994. Genomic structure and chromosomal localisation of processed pseudogenes for human RBP-Jk. Jpn. J. Hum. Genet. 39, 393–401.
Zhao, Q., Dobbs-McAuliffe, B., Linney, E., 2005. Expression of cyp26b1 during zebrafish early development. Gene Expr. Patterns 3, 363–369.